



Research paper

# Novel neuroprotective 5,6-dihydropyrido[2',1':2,3]imidazo[4,5-c]quinoline derivatives acting through cholinesterase inhibition and CB2 signaling modulation

Sushovan Jena<sup>a,1</sup>, Gabriel Gonzalez<sup>b,c,1</sup>, Dominik Vítek<sup>d</sup>, Marie Kvasnicová<sup>b,f</sup>, Šárka Štěpánková<sup>e</sup>, Miroslav Strnad<sup>f</sup>, Jiří Voller<sup>b,d,\*</sup>, Kaushik Chanda<sup>g,\*\*</sup>

<sup>a</sup> Department of Chemistry, School of Advanced Sciences, Vellore Institute of Technology, Vellore, Tamil Nadu, 632014, India

<sup>b</sup> Department of Experimental Biology, Palacky University Olomouc, Faculty of Science, Šlechtitelů 27, 78371, Olomouc, Czech Republic

<sup>c</sup> Department of Neurology, University Hospital in Olomouc, I. P. Pavlova 6, 77520, Olomouc, Czech Republic

<sup>d</sup> Institute of Molecular and Translational Medicine, Faculty of Medicine and Dentistry, Palacký University, Hněvotínská 5, 77515, Olomouc, Czech Republic

<sup>e</sup> Department of Biological and Biochemical Sciences, Faculty of Chemical Technology, University of Pardubice, Studentská 573, 53210, Pardubice, Czech Republic

<sup>f</sup> Laboratory of Growth Regulators, Faculty of Science, Palacký University Olomouc, and Institute of Experimental Botany of the Czech Academy of Sciences, Šlechtitelů 27, CZ-78371, Olomouc, Czech Republic

<sup>g</sup> Department of Chemistry, Rabindranath Tagore University, Hojai, Assam, 782435, India

## ARTICLE INFO

## Keywords:

One-pot synthesis  
Telescopic approach  
Microwave-assisted synthesis  
Neurodegeneration  
Mitochondria  
Choline esterase  
Parkinson's disease

## ABSTRACT

A novel group of 5,6-dihydropyrido [2',1':2,3]imidazo [4,5-c]quinolines was prepared via a microwave assisted one-pot telescopic approach. The synthetic sequence involves the formation of an amine precursor of imidazo [1,2-a]pyridine via condensation and reduction under microwave irradiation. Subsequently, the Pictet-Spengler cyclisation reaction occurs with ketones (cyclic or acyclic) to obtain substituted 5,6-dihydropyrido [2',1':2,3]imidazo [4,5-c]quinolines in excellent yields. The compounds were tested as neuroprotective agents. Observed protection of neuron-like cells, SH-SY5Y differentiated with ATRA, in Parkinson's and Huntington's disease models inspired further mechanistic studies of protective activity against damage induced by 1-methyl-4-phenylpyridinium (MPP+), a compound causing Parkinson's disease. The novel compounds exhibit similar or higher potency than ebselen, an established drug with antioxidant activity, in the cells against MPP + -induced total cellular superoxide production and cell death. However, they exhibit a significantly higher capacity to reduce mitochondrial superoxide and preserve mitochondrial membrane potential. We also observed marked differences between a selected derivative and ebselen in terms of normalizing MPP + -induced phosphorylation of Akt and ERK1/2. The cytoprotective activity was abrogated when signaling through cannabinoid receptor CB2 was blocked. The compounds also inhibit both acetylcholine and butyrylcholine esterases. Overall the data show that novel 5,6-dihydropyrido [2',1':2,3]imidazo [4,5-c]quinoline have a broad cytoprotective activity which is mediated by several mechanisms including mitoprotection.

## 1. Introduction

Neurodegenerative diseases represent the second largest group of civilization disorders. Parkinson's disease (PD) is the most common motor-related disease, characterized by symptoms such as bradykinesia, rigidity, and tremor, which manifest after the loss of approximately 50–80 % of dopaminergic neurons in the *Substantia nigra pars compacta*.

Currently, PD is experiencing a dramatic increase, with prevalence of about 1 % in the population over 60 years old. Despite the increasing understanding of PD susceptibility genetics (polymorphisms in PINK1, LRRK2, DJ1, and other genes), the sporadic form of PD (without an identified cause) predominates in the newly diagnosed cases of the disorder. Cellular and molecular hallmarks of sporadic PD include proteasomal and autophagy-lysosomal dysfunction associated with synucleinopathy [1,2], high oxidative stress [3], mitochondrial dysfunction

\* Corresponding author. Department of Experimental Biology, Palacky University Olomouc, Faculty of Science, Šlechtitelů 27, 78371, Olomouc, Czech Republic.

\*\* Corresponding author.

E-mail addresses: [jiri.voller@upol.cz](mailto:jiri.voller@upol.cz) (J. Voller), [chandakaushik1@gmail.com](mailto:chandakaushik1@gmail.com), [kaushikchanda@rtuassam.ac.in](mailto:kaushikchanda@rtuassam.ac.in) (K. Chanda).

<sup>1</sup> Contributed equally for the manuscript.

### List of abbreviations

AChE	acetylcholinesterase
ATRA	all- <i>trans</i> retinoic acid
BChE	butyrylcholinesterase
ChEI	cholinesterase inhibitor
DMSO	dimethylsulphoxide
EBS	ebesen
HD	Huntington's disease
LDH	lactate dehydrogenase
NAC	<i>N</i> -acetylcysteine
3-NPA	3-nitropropionic acid
PD	Parkinson's disease
PI	propidium iodide
MPP+	1-methyl-4-phenylpyridinium
MW	microwaves

[4], microglia- and astrocyte-mediated neuroinflammation [5]. The current PD therapies alleviate symptoms but do not prevent disease progression [6,7]. One of the disease-modifying strategies is pharmacological prevention of further neurodegeneration. The neuroprotective effects of various compounds have been reported in both *in vitro* and *in vivo* PD models [8–17]. However, despite the significant drug discovery efforts, no disease-modifying agent has been approved for PD treatment, emphasizing the need for novel therapeutics.

Although the importance of ACh level maintenance has been mainly discussed in relation to Alzheimer's disease, cholinesterase inhibitors (ChEI) have also been studied as drugs for Parkinson's disease dementia [18] with indirect protective effect through modulation of neuro-inflammatory processes and the ability to induce neurogenesis [19]. Several studies by us and others have already demonstrated beneficial effects of butyrylcholinesterase (BChE) inhibition in Parkinson's disease models [20–22]. Inhibition of BChE is associated with the improved cognitive functions in various dementia diseases through increasing acetylcholine levels, *anti*-neuroinflammatory activity and prevention of  $\beta$ -amyloid aggregation [23,24]. In contrast to acetylcholinesterase (AChE) inhibition, which is a well-known treatment strategy for Alzheimer disease (AD), PD and other dementia, BChE inhibition has not been linked with cardiac side effects [25]. Currently, the cholinesterase inhibitors are the only small molecule drugs able to enhance cognitive and functional symptoms associated with neurodegenerative diseases in patients [26].

Another class of promising neuroprotective compounds is ligands of G-protein coupled CB1 and CB2 cannabinoid receptors. Particularly interesting are CB2 ligands (mainly agonists) that offer both direct and indirect neuroprotective activity through anti-inflammatory effect without the psychoactive activity observed in CB1 ligands [27,28].

Currently, many other possible approaches to protect neuronal cells from oxidative stress are under investigation [29,30]. Studied scaffolds include quinolones structurally related to antibacterial chemotherapeutics targeting bacterial gyrase. Notably, a signaling molecule from the bacterial quorum-sensing system, 2-heptyl-3-hydroxy-4(1H)-quinolone (A), has been also reported to protect the neuronal cells *in vitro* by inhibiting cellular  $Ca^{2+}$  uptake inhibition and preventing ROS accumulation [31]. The neuroprotective effects of 2(1H)-quinolone derivatives (B) have been demonstrated in gerbil global ischemia model [32]. Additionally, the quinolone fisetin analogs (C) have neuroprotective effects *in vitro* models [33]. Finally, some quinolinone derivatives (D, E) are both potent CB2 agonists [34] and ChEI [35]. Compound (F) has been identified as a novel selective ligand for cannabinoid CB2 receptor [36].

In this study, a library of novel 5,6-dihydropyrido [2',1':2,3]imidazo [4,5-*c*]quinoline derivatives was synthesized using one-pot microwave

assisted telescopic approach. Recently, one-pot telescopic approach gained immense importance for the synthesis of bioactive compounds or medicines [37,38]. The main advantage of one-pot telescopic approach is that it avoids the need of separation and purification of reaction intermediates and uses a better yielding, time-saving practice. The synthesized compounds were subsequently evaluated for neuroprotection in *in vitro* models relevant for PD and Huntington's disease in human neuron-like SH-SY5Y cells. The evaluation of activity in this panel of neurodegeneration-related assays was inspired by the results of a high-throughput screening for cytoprotective activity in skin cells, where one of the derivatives emerged among the top hits and was subsequently validated (Supplementary figure S1). The most promising compounds were then assessed for their inhibitory activity on cholinesterases and their ability to modulate CB2 receptor signaling. For BChE molecular target, we compared their binding mode with known ChEI using molecular docking.

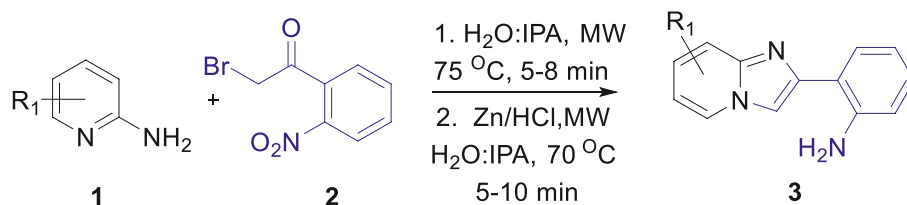
Overall, the combined anti-cholinesterase activity, which should lead to symptom relieve, and disease modifying neuroprotective activity *via* CB2 signaling modulation may present an improved therapeutical potential in comparison with single-mode-of-action agents.

## 2. Results and discussion

### 2.1. Chemistry

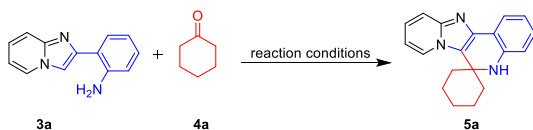
Our initial synthetic strategy is shown in Scheme 1 to obtain the target compound 5,6-dihydropyrido [2',1':2,3]imidazo [4,5-*c*]quinoline derivatives 5. To evaluate the practicability of our proposed synthetic manipulation, we first developed the precursor material, substituted 2-(imidazo [1,2-*a*]pyridin-2-yl)aniline 3 in one-pot step using our reported procedure (Scheme 1) [39]. Initially, the reaction of substituted 2-aminopyridine 1 with 2-bromo-2'-nitroacetophenone 2 using microwaves under green media resulted the synthesis of substituted 2-(2-nitrophenyl)imidazo [1,2-*a*]pyridine which upon reduction with Zn dust/HCl under microwaves resulted the formation of 2-(imidazo [1,2-*a*]pyridin-2-yl)aniline 3 in one-pot pathway.

Next, we started our probe for the Pictet–Spengler cyclisation reaction as an important and powerful tool for ecologically benign, economically attractive syntheses of fused polycyclic heteroarenes. In the Pictet–Spengler cyclisation reaction, an activated or unactivated aryl amine and carbonyl substrates first react to produce an imine intermediate, which is then converted into the cyclized product through a 6-endo intramolecular cyclisation. In this pursuit, we choose 2-(imidazo [1,2-*a*]pyridin-2-yl)aniline 3a and cyclohexanone 4a as model substrates for the optimization studies. Here we choose  $CF_3COOH$  as an acid catalyst. The results are summarized in Table 1. The reaction of compound 3a with cyclohexanone 4a under neat condition at room temperature using  $CF_3COOH$  as an acid catalyst did not yield the cyclized product 5a (Table 1, entry 1). Further heating the reaction mixture for 6 h at 80 °C yielded the cyclized product 5a in 20 % yield (Table 1, entry 2). Replacing the reaction solvent with  $CHCl_3$  under refluxing condition for 6 h led to the formation of cyclized product 5a in 75 % yield (Table 1, entry 3). Subsequently, to enhance the product yield switching the reaction solvent DMSO under identical reaction condition led to either low efficiency or a failure to promote the transformations (Table 1, entry 4). Performing the cyclisation reaction under polar protic solvents such as refluxing MeOH, or isopropanol failed to enhance the product yield (Table 1, entries 5, 6). Switching from polar protic solvents, to mixed solvents such water and isopropanol in (1:1) ratio, surprisingly increase the yield of product 5a to 80 % upon heating at 80 °C (Table 1, entry 7). Subsequently, upon applying the microwave irradiation at 70 °C for 10 min under identical condition resulted an excellent yield of the product 5a in 92 % (Table 1, entry 8). However, using  $CHCl_3$  as a reaction mixture under microwave irradiation did not enhance the yield of the product 5a to substantial amount (Table 1, entry 9). This microwave assisted reaction for the synthesis of diverse 5,6-dihydropyrido



**Scheme 1.** Synthesis of 2-(imidazo [1,2-a]pyridin-2-yl)aniline derivatives **3**.

**Table 1**  
Optimization of Heterocyclisation Reaction Conditions.<sup>a</sup>



Entry	Solvent	Acid catalyst	Temperature	Time	Yield (%) <sup>c</sup>
1	Neat	CF <sub>3</sub> COOH	rt	6 h	0
2	Neat	CF <sub>3</sub> COOH	60 °C	6 h	20
3	CHCl <sub>3</sub>	CF <sub>3</sub> COOH	reflux	6 h	75
4	DMSO	CF <sub>3</sub> COOH	80 °C	6 h	40
5	MeOH	CF <sub>3</sub> COOH	reflux	6 h	60
6	IPA	CF <sub>3</sub> COOH	reflux	6 h	70
7	H <sub>2</sub> O-IPA	CF <sub>3</sub> COOH	80 °C	6 h	80
8	H <sub>2</sub> O-IPA	CF <sub>3</sub> COOH	MW <sup>b</sup> , 70 °C	10 min	92
9	CHCl <sub>3</sub>	CF <sub>3</sub> COOH	MW <sup>b</sup> , 70 °C	10 min	85

<sup>a</sup> Reaction was performed using **3a** (1 mmol), **4a** (1.1 mmol), CF<sub>3</sub>COOH (1 mmol).

<sup>b</sup> Microwave reactions were carried out in Microwave Model No. CATA R (Catalyst systems, Pune) using power 280 W.

<sup>c</sup> Yield of the isolated product.

[2',1':2,3]imidazo [4,5-c]quinoline derivatives was subsequently explored under optimal conditions (Table 1, entry 8).

After successfully executing the dihydropyrido [2',1':2,3]imidazo [4,5-c]quinoline ring formation **5**, our next attempt was to obtain the synthetic manipulation in a one-pot telescoped manner. Next, we performed one-pot telescoped reaction where the reaction of substituted 2-aminopyridine **1** with 2-bromo-2-nitroacetophenone **2** under microwave irradiation for 5–8 min at 75 °C in water/IPA solvent resulted substituted 2-(2-nitrophenyl)imidazo [1,2-a]pyridine which upon reduction under acidic condition with microwaves resulted the formation of 2-(imidazo [1,2-a]pyridin-2-yl)aniline **3**. Without isolating the intermediate product **3**, same reaction mixtures were irradiated under microwaves for 10–15 min at 70 °C with *in-situ* addition of substituted ketones and TFA to obtain the desired dihydropyrido [2',1':2,3]imidazo [4,5-c]quinoline derivatives as depicted in Scheme 2.

Upon completion of the reaction, the <sup>1</sup>H NMR spectrum of the

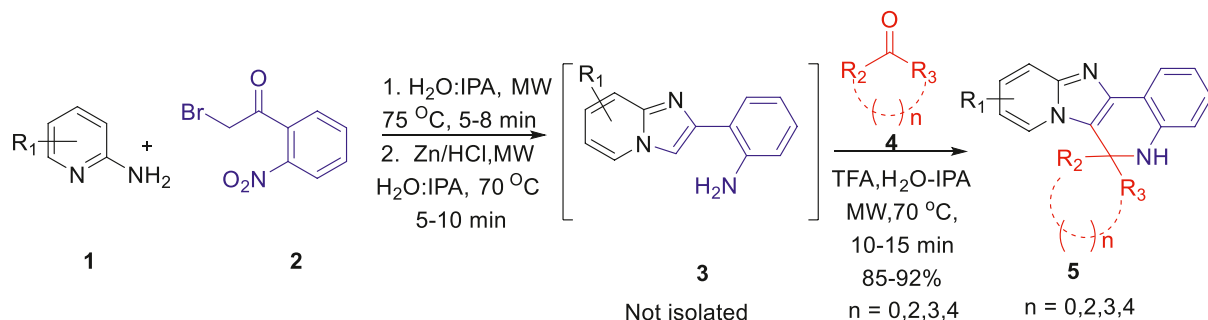
synthesized compound indicated the formation of pure dihydropyrido [2',1':2,3]imidazo [4,5-c]quinoline derivatives **5** in excellent yield. Next, we expanded the substrate scope to include different electron donating and electron withdrawing substituents on 2-aminopyridine substrate in order to further assess the effectiveness of this one-pot telescopic technique and to swiftly increase our unique chemical library. As depicted in Scheme 3, we could find a smooth transformation of substituted 2-aminopyridine to unique dihydropyrido [2',1':2,3]imidazo [4,5-c]quinoline moieties in excellent yields. Finally, the corresponding dihydropyrido [2',1':2,3]imidazo [4,5-c]quinoline moieties **5** were successfully produced after the telescoping reaction with excellent yields. This was followed by straightforward work-up procedures that included removal of solvent under reduced pressure, extraction, and solvent evaporation. Finally, the pure products were obtained by trituration without using column chromatography, which was followed by the spectroscopic analysis of the pure compounds using <sup>1</sup>HNMR, <sup>13</sup>C NMR, mass (MS), and IR spectroscopy.

To further confirm dihydropyrido [2',1':2,3]imidazo [4,5-c]quinoline moieties **5**, we undertook the X-ray crystallographic study of compound **5f**. Fig. 2 depicts the ORTEP diagram of compound **5f** with salt form of trifluoroacetic acid (X-ray crystallographic data were specified in Supporting Information). The X-ray crystal structure of compound **5f** indicates that pyridyl group and quinoline moiety are present in the same plane with exclusive dihydropyrido [2',1':2,3]imidazo [4,5-c]quinoline ring formation [40].

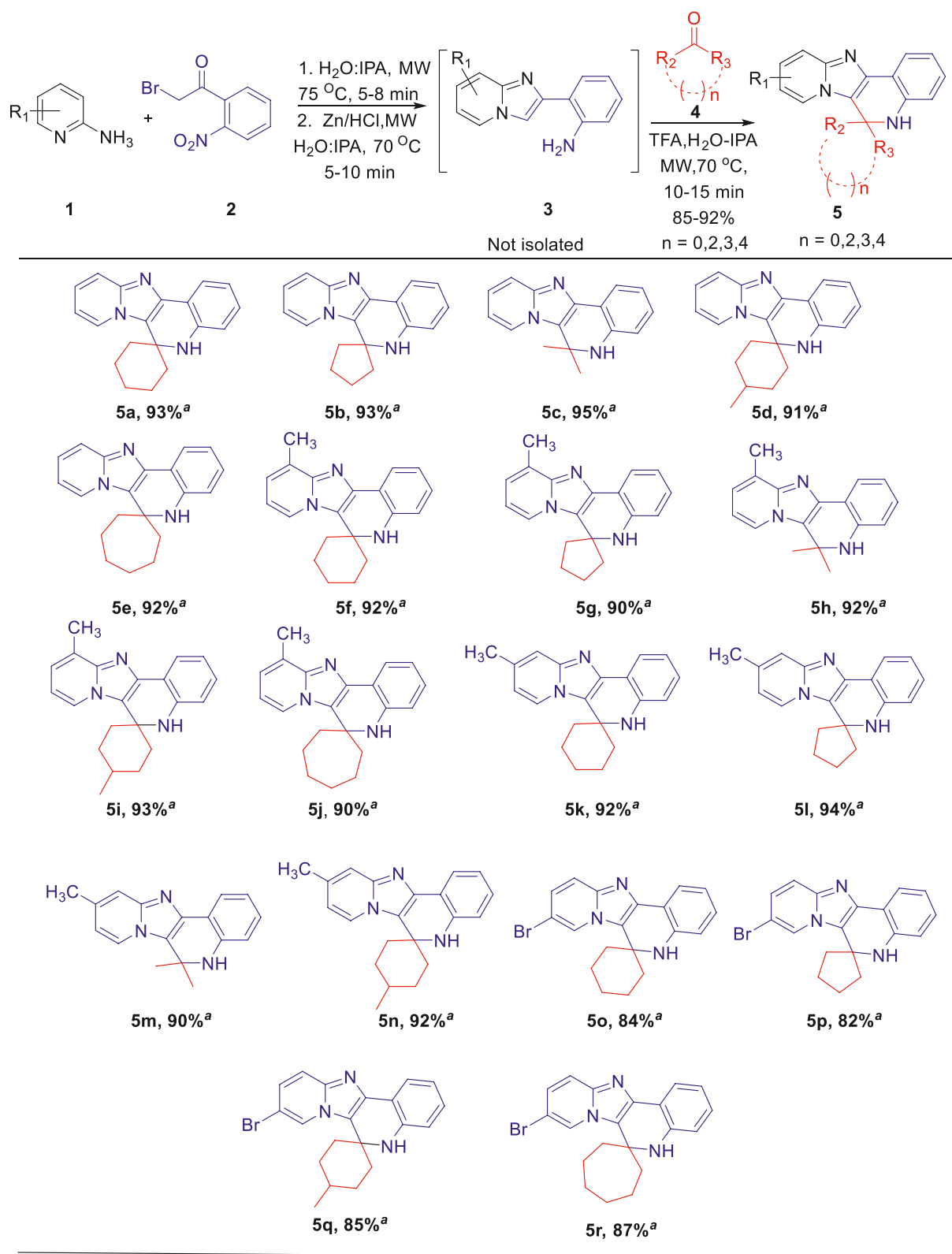
## 2.2. Biology

### 2.2.1. The effect of novel quinoline derivatives on the cytotoxicity of neuron-like SH-SY5Y cells

The neurotoxicity assessment of the novel derivatives is a key parameter for follow-up neuroprotection studies. For this purpose, the neuron-like phenotype of SH-SY5Y cells was induced by 10 μM all-*trans* retinoic acid (ATRA) for 48 h and then the cells were exposed to the test compounds for 72 h. The cytotoxicity was measured by propidium iodide (PI) exclusion assay [41]. Triton X-100 (1 %) was used as a standard (set as 100 % cytotoxicity). As shown in Table 2, the compounds did not display significant toxic effect which was defined as a 10 % surplus of cell death above DMSO control (14.5 ± 0.6 %).



**Scheme 2.** Microwave-assisted one-pot telescoped approach to dihydropyrido [2',1':2,3]imidazo [4,5-c]quinoline derivatives **5** in green media.



**Scheme 3.** Microwave-assisted one-pot telescopic approach to dihydropyrido [2,1':2,3]imidazo [4,5-c]quinoline derivatives **5** in green media. <sup>a</sup> Denotes the isolated yields.

### 2.2.2. The neuroprotective effect in 3-nitropropionic acid- and MPP<sup>+</sup>-induced neurodegeneration models in the neuron-like SH-SY5Y cells

Since mitochondria dysfunction is a key pathological feature in neurodegenerations, an evaluation of the protection of SH-SY5Y cells

differentiated by ATRA treatment against mitochondria-targeting toxins 3-nitropropionic acid (3-NPA) and 1-methyl-4-phenylpyridinium (MPP<sup>+</sup>) was performed using PI exclusion assay. 3-NPA is an agent used to mimic Huntington's Disease (HD) in rodents and *in vitro* by

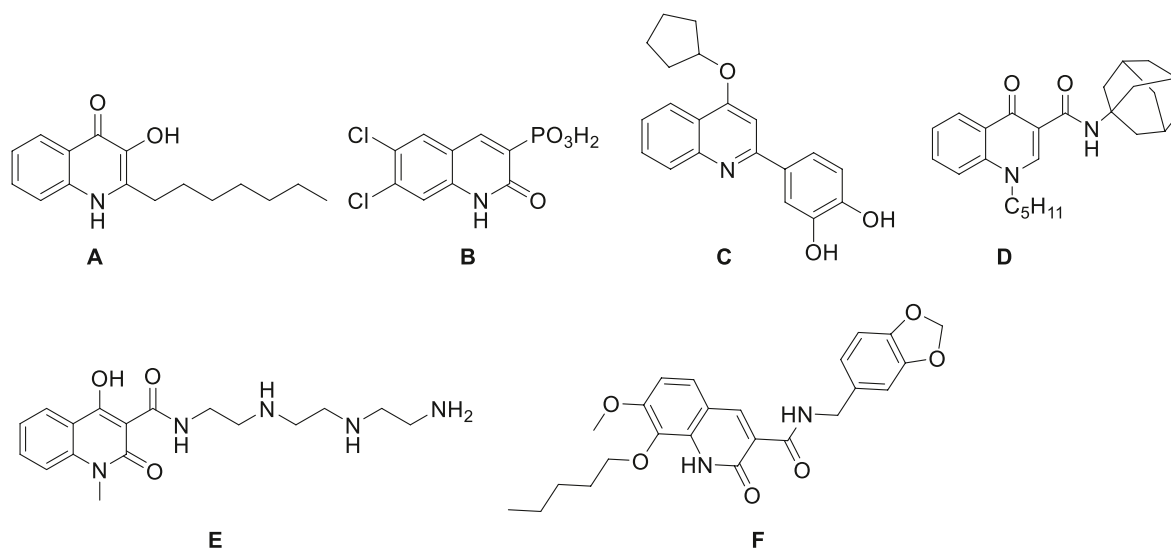


Fig. 1. Quinoline derivatives with neuroprotective activity and/or affinity towards CB2 receptors or cholinesterases.

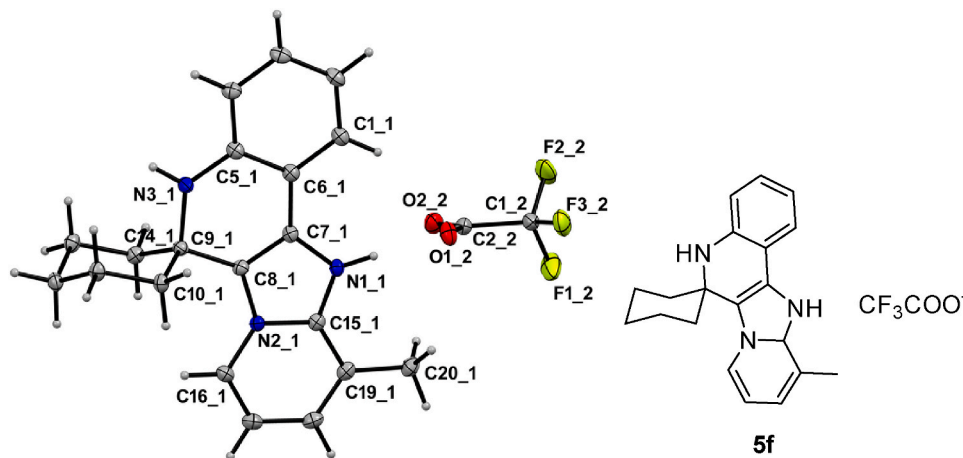


Fig. 2. ORTEP diagram of compound **5f** with 50 % thermal ellipsoid probability.

selectively damaging mitochondria through the irreversible inhibition of complex II of the respiratory chain which results in the opening of mitochondrial permeability transition pores and apoptosis (of striatal neurons). The neuron-like SH-SY5Y cells were co-treated by the studied compounds and 20 mM 3-NPA for 48 h. The antioxidant *N*-acetylcysteine (NAC) was used as a positive control [41]. When the PI signal of 3-NPA-treated cells was set to 100 %, the corresponding signal of DMSO-treated control cells was  $25.5 \pm 1.2$  %.

As shown in Table 2, most of the compounds in concentrations between 1 and 10  $\mu$ M reduced cell death by 20–50 %. NAC demonstrated a stronger protective effect (around 63 %), however it was achieved only at concentrations 2–3 orders of magnitude higher. Surprisingly, the second positive control ebselen (EBS), a well-known cytoprotective and anti-inflammatory agent active in multiple *in vitro* neurodegeneration or stress models [42,43], did not show any protective effect in our 3-NPA model and even increased proportion of dead cells.

The other studied mitochondrial toxin MPP+ is well-known inducer of PD. It enters dopaminergic neurons through dopamine transporter and inhibits electron transport chain complex I. Disruption of ATP production and oxidative stress results in apoptosis or necroptosis [44,45]. MPP+ can also cause oxidative stress by increasing dopamine levels in the cytosol, which leads to the production of dopamine-derived quinones [46]. The MPP+ -treated dopaminergic SH-SY5Y cell line is

widely used as a model to evaluate the effectiveness of neuroprotective agents for potential treatments of sporadic PD [47]. In this study, ATRA-differentiated SH-SY5Y cells were co-treated with the compounds and 5 mM MPP+ for 24 h. The results are summarized in Table 2. Once again, PI signal of MPP+ -treated cells was set to 100 %. The corresponding value for DMSO-treated control cells was  $33.8 \pm 1.5$  %. EBS, used as positive control, showed complete neuroprotection at 10  $\mu$ M. Comparably robust neuroprotective effect was observed for the majority of derivatives. Specifically, **5a**, **5b**, **5c**, **5e**, **5j**, **5k**, **5l**, **5n**, **5o** and **5p** decreased MPP+ -induced cell death completely, reaching the values of control. Whereas derivatives **5c** and **5p** showed dose-dependent activity other derivatives were most active at 10  $\mu$ M. Based on these observations, compounds **5a**, **5c**, **5k**, **5o** and **5p** were selected for further more detailed study in MPP+ model.

### 2.2.3. Novel quinoline derivatives exert robust neuroprotective and anti-apoptotic effects against MPP+ toxicity

As mentioned above, MPP+ is potent inducer of cell death and similarly to other PD-inducing toxins activates apoptosis in neurons. Based on the complete protection of SH-SY5Y neuron-like cells by compounds **5a**, **5c**, **5k**, **5o**, and **5p** in the MPP+ model, these derivatives were selected for further activity validation in the same system. After confirming their neuroprotective activity using the orthogonal lactate

**Table 2**

Effect of the novel 5,6-dihydropyrido [2,1':2,3]imidazo [4,5-c]quinoline derivatives on cytotoxicity, protective effect in 3-nitropropionic acid- and MPP + -induced cell death of neuron-like SH-SY5Y cells.

Compound	Cytotoxicity Cell death (%) <sup>a</sup>	3-NPA model Cell death (%) <sup>b</sup>			MPP + model Cell death (%) <sup>b</sup>		
	10 $\mu$ M	0.1 $\mu$ M	1 $\mu$ M	10 $\mu$ M	0.1 $\mu$ M	1 $\mu$ M	10 $\mu$ M
<b>5a</b>	12.2 $\pm$ 1.0	78.5 $\pm$ 4.7	64.0 $\pm$ 4.5	65.8 $\pm$ 3.0	57.0 $\pm$ 9.3	37.3 $\pm$ 5.3	52.7 $\pm$ 3.9
<b>5b</b>	10.1 $\pm$ 0.4	67.7 $\pm$ 5.2	57.7 $\pm$ 4.0	54.5 $\pm$ 2.7	63.9 $\pm$ 7.0	28.2 $\pm$ 3.9	42.6 $\pm$ 4.6
<b>5c</b>	14.6 $\pm$ 0.9	98.7 $\pm$ 7.1	83.1 $\pm$ 5.1	57.8 $\pm$ 2.9	96.7 $\pm$ 10.7	39.7 $\pm$ 5.0	26.2 $\pm$ 4.3
<b>5d</b>	12.0 $\pm$ 0.9	82.3 $\pm$ 6.5	64.2 $\pm$ 2.7	64.5 $\pm$ 3.5	67.6 $\pm$ 8.0	33.6 $\pm$ 5.7	97.3 $\pm$ 6.3
<b>5e</b>	10.4 $\pm$ 0.8	74.0 $\pm$ 3.0	69.9 $\pm$ 4.3	69.0 $\pm$ 4.6	45.8 $\pm$ 5.0	28.6 $\pm$ 6.0	73.6 $\pm$ 10.8
<b>5f</b>	9.2 $\pm$ 0.5	76.6 $\pm$ 8.0	66.1 $\pm$ 3.2	61.8 $\pm$ 3.4	77.7 $\pm$ 6.7	44.4 $\pm$ 5.8	45.6 $\pm$ 5.3
<b>5g</b>	8.2 $\pm$ 0.6	79.2 $\pm$ 5.2	65.3 $\pm$ 5.0	60.5 $\pm$ 4.0	86.7 $\pm$ 5.2	48.0 $\pm$ 5.06	52.8 $\pm$ 7.9
<b>5h</b>	11.0 $\pm$ 0.8	96.6 $\pm$ 4.2	69.9 $\pm$ 5.3	56.4 $\pm$ 4.4	79.6 $\pm$ 7.6	48.6 $\pm$ 4.7	70.8 $\pm$ 4.5
<b>5i</b>	9.0 $\pm$ 0.8	86.0 $\pm$ 7.0	65.0 $\pm$ 4.0	64.5 $\pm$ 4.0	91.8 $\pm$ 10.8	53.0 $\pm$ 3.5	94.0 $\pm$ 8.2
<b>5j</b>	9.3 $\pm$ 0.7	83.8 $\pm$ 4.9	71.0 $\pm$ 2.8	60.3 $\pm$ 4.7	67.2 $\pm$ 5.5	38.8 $\pm$ 4.3	91.4 $\pm$ 7.8
<b>5k</b>	11.4 $\pm$ 1.0	75.5 $\pm$ 6.0	62.6 $\pm$ 2.4	55.2 $\pm$ 5.0	60.8 $\pm$ 4.9	38.2 $\pm$ 3.6	75.0 $\pm$ 5.5
<b>5l</b>	10.4 $\pm$ 1.0	86.9 $\pm$ 5.9	59.0 $\pm$ 3.3	48.6 $\pm$ 2.9	73.1 $\pm$ 6.1	31.9 $\pm$ 6.2	68.9 $\pm$ 6.0
<b>5m</b>	13.0 $\pm$ 1.6	86.2 $\pm$ 5.4	62.4 $\pm$ 2.7	52.9 $\pm$ 2.7	65.7 $\pm$ 6.5	46.1 $\pm$ 2.9	59.7 $\pm$ 4.4
<b>5n</b>	10.9 $\pm$ 1.6	82.4 $\pm$ 4.7	66.8 $\pm$ 2.6	67.0 $\pm$ 3.5	61.6 $\pm$ 5.5	38.4 $\pm$ 3.6	105.9 $\pm$ 7.7
<b>5o</b>	12.3 $\pm$ 0.9	97.7 $\pm$ 3.0	88.4 $\pm$ 6.3	59.5 $\pm$ 3.7	94.8 $\pm$ 8.4	56.5 $\pm$ 3.3	33.9 $\pm$ 3.6
<b>5p</b>	12.2 $\pm$ 1.2	78.4 $\pm$ 3.5	63.9 $\pm$ 2.3	59.7 $\pm$ 2.6	66.4 $\pm$ 5.2	31.8 $\pm$ 4.5	27.5 $\pm$ 3.8
<b>5q</b>	9.3 $\pm$ 1.4	92.1 $\pm$ 5.3	71.3 $\pm$ 4.7	64.0 $\pm$ 5.5	74.2 $\pm$ 4.1	52.3 $\pm$ 2.7	126.5 $\pm$ 12.3
<b>5r</b>	13.5 $\pm$ 1.8	90.7 $\pm$ 4.0	81.4 $\pm$ 2.5	73.5 $\pm$ 7.1	56.5 $\pm$ 3.3	43.5 $\pm$ 3.2	96.40 $\pm$ 11.4
EBS	18.3 $\pm$ 1.8	118.7 $\pm$ 7.3	112.0 $\pm$ 4.9	132.9 $\pm$ 16.2	99.5 $\pm$ 11.9	80.0 $\pm$ 9.8	27.5 $\pm$ 4.8
NAC <sup>c</sup>	n.d.	95.5 $\pm$ 5.9	80.8 $\pm$ 6.9	37.0 $\pm$ 3.1	n.d.	n.d.	n.d.

The values represent the averages of at least three independent experiments conducted on separate days.

<sup>a</sup> The effect of Triton X 100 was set to 100 %, the value for DMSO vehicle was 14.5  $\pm$  0.6 %.

<sup>b</sup> The effect of the toxin was set to 100 %. The DMSO vehicle values were 25.5  $\pm$  1.2 % and 33.8  $\pm$  1.5 % for the 3-NPA and MPP + models, respectively.

<sup>c</sup> Tested in concentration 10, 100 and 1000  $\mu$ M.

dehydrogenase (LDH) release toxicity assay, the compounds were evaluated for their effect on apoptosis through YOPRO-1 staining and caspase-3/7 activity assay. Values of these parameters for the MPP + treated cells were set to 100 %.

The results of LDH release assay (Fig. 3A) demonstrate that the treatment with MPP + increases cell death 2.5 times in comparison with DMSO control cells (40.4  $\pm$  3.3 %). Co-treatment with 10  $\mu$ M EBS significantly reduced LDH signal to 59.2  $\pm$  5.3 %. In comparison, compounds **5a** (1  $\mu$ M), **5k** (1  $\mu$ M) and **5o** (10  $\mu$ M) demonstrated slightly weaker activity, as indicated by LDH signal levels of 65.1  $\pm$  8.0 %, 65.4  $\pm$  6.7 % and 64.7  $\pm$  6.3 %, respectively. On the other hand, derivatives **5c** and **5p** at 10  $\mu$ M displayed numerically superior neuroprotective effects when compared to EBS, with cytotoxicity levels of 50.2  $\pm$  4.9 % and 51.9  $\pm$  4.9 %, respectively. Additionally, both derivatives exhibited a significant decrease in cell death even at a concentration of 1  $\mu$ M. Notably, the effect of 1  $\mu$ M **5p** (58.5  $\pm$  3.9 %) was comparable to that of 10  $\mu$ M EBS.

Furthermore, anti-apoptotic effect of selected derivatives in the MPP + model was studied by two apoptosis-related assays YOPRO-1 nuclear staining and caspase-3,7 (casp-3,7) activation assays. Fluorescent YOPRO-1, in contrast to PI, stains early apoptotic cells. In YOPRO-1 assay (Fig. 3B), MPP + induced a 3-fold increase in proportion of apoptotic cells compared to DMSO control (28.8  $\pm$  1.6 %).

EBS at 10  $\mu$ M reduced apoptosis to 53.4  $\pm$  3.8 %. The novel derivatives showed comparable or better anti-apoptotic effect often at 1  $\mu$ M as shown in Fig. 3B, accounting for 1  $\mu$ M **5a** (58.7  $\pm$  2.7 %), 1–10  $\mu$ M **5c** (58.8  $\pm$  3.3 %; 37.9  $\pm$  2.0 %), 1  $\mu$ M **5k** (58.1  $\pm$  2.2 %), 10  $\mu$ M **5o** (58.0  $\pm$  4.0 %) and 1–10  $\mu$ M **5p** (47.3  $\pm$  2.7 %; 43.5  $\pm$  3.0 %), respectively. The anti-apoptotic activity of the most active derivatives **5c** and **5p** was also confirmed by confocal microscopy (see Fig. 3D). Control cells showed no YO-PRO1 signal and MPP + treatment induced a significant increase. As expected, co-treatment with the compounds resulted in a marked reduction of YOPRO-1 positive cells fluorescence.

Strong anti-apoptotic effect of the compounds was also observed in casp-3,7 activity assay (see Fig. 3C), where they blunted the 5-fold increase after MPP + treatment in comparison to DMSO control cells (20.4

$\pm$  1.0 %). The co-treatment with 10  $\mu$ M EBS showed dramatic decrease to 36.3  $\pm$  1.6 %. The casp-3,7 signals relative to MPP + treated cells were as follows for **5a** (1  $\mu$ M, 59.1  $\pm$  2.6 %), **5c** (1  $\mu$ M, 64.2  $\pm$  2.9 %; 10  $\mu$ M, 48.8  $\pm$  1.5 %), **5k** (1  $\mu$ M, 52.6  $\pm$  3.2 %), **5o** (10  $\mu$ M, 55.8  $\pm$  2.7 %), and **5p** (1  $\mu$ M, 49.4  $\pm$  1.4 %; 10  $\mu$ M, 72.6  $\pm$  2.4 %).

Finally, **5c** was selected for further confirmation of apoptotic changes by immunodetection of PARP1 and its cleavage fragment. As shown in Fig. 5B, MPP + induced PARP1-cleavage, whereas **5c** and EBS decreased PARP1 fragment levels. These data correlate with assays described above.

### 2.3. Novel quinoline derivatives attenuate both cellular and mitochondrial production of superoxide radicals induced by MPP+

The toxic effect of MPP + on mitochondria and induction oxidative stress was described above. However, MPP + can also induce oxidative stress also by other mechanisms such as inducible NO synthase [48,49] and NADPH-oxidase [50]. The comparable neuroprotective effects of the compounds **5a**, **5c**, **5k**, **5o** and **5p** and the antioxidant and glutathione-peroxidase mimetic EBS prompted us to investigate the effect on cellular and mitochondrial superoxide radicals using dihydroethidium (DHE) and MitoSOX assays, respectively. Similarly to the assays above, the resulting effect of MPP+ was set to 100 % (Fig. 4A).

Compared to DMSO control (35.8  $\pm$  2.5 %), cellular superoxide radicals production was elevated almost 3-times by MPP + treatment. At a concentration of 10  $\mu$ M, EBS reduced cellular superoxide radical levels to 57.1  $\pm$  1.7 %. However, compounds **5c** and **5p** outperformed this effect, with reductions in cellular superoxide of 44.4  $\pm$  2.6 % and 52.2  $\pm$  3.0 %, respectively. The other derivatives exhibited lower efficiency, with reductions of 59.9  $\pm$  2.6 % (1  $\mu$ M **5a**), 67.1  $\pm$  2.8 % (1  $\mu$ M **5k**) and 65.6  $\pm$  2.9 % (10  $\mu$ M **5o**).

Notably, MitoSOX staining showed even more pronounced effect of MPP + treatment on mitochondrial superoxide radicals production with levels increased more than 3.7-times in comparison with controls cells (26.8  $\pm$  3.0 %) as shown in Fig. 4B.

While 10  $\mu$ M EBS efficiently reduced total cellular superoxide as

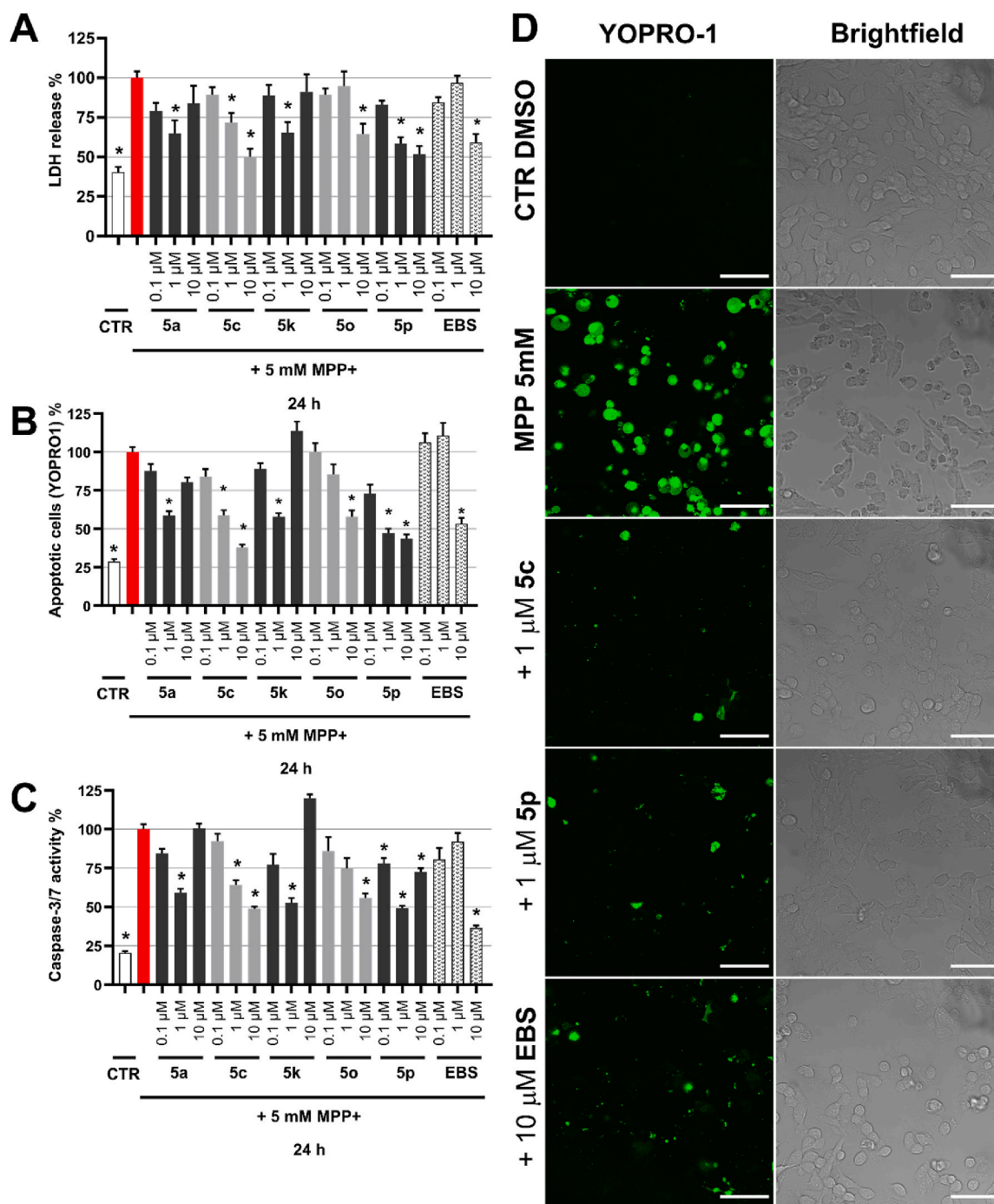


**Fig. 3.** A) Neuroprotective effect of derivatives **5a-p** and ebselen on MPP + -induced toxicity in neuron-like SH-SY5Y cells as measured by LDH assay. B) Anti-apoptotic effect of derivatives **5a-p** and ebselen in the MPP + -induced toxicity on neuron-like SH-SY5Y cells evaluated by YOPRO1 staining. C) MPP + -induced caspase-3,7 activation and protective effect of **5a-p** and ebselen in the model. The experiments were conducted in triplicate on at least three independent days. The asterisks designate statistically significant comparisons ( $P < 0.05$ ) with the sample treated with 5 mM MPP+. D) Representative fluorescence microphotographs of YOPRO-1-stained neuron-like SH-SY5Y. The bar = 50 μm.

mentioned earlier, its effect on mitochondrial superoxide was much less pronounced ( $63.3 \pm 5.3\%$ ). Similarly, activity was observed for 1 μM compound **5a** ( $61.7 \pm 3.2\%$ ) and 10 μM compound **5o** ( $58.8 \pm 6.2\%$ ), respectively. However, the most active compounds, **5c** and **5p**, clearly outperformed EBS at 10 μM, achieving reductions in mitochondrial superoxide to  $41.3 \pm 4.3\%$  and  $41.3 \pm 6.2\%$ , respectively. Compound **5k** did not exhibit a significant activity. On the other hand, the most active compounds **5c** and **5p** at 10 μM completely outperformed EBS, reaching  $41.3 \pm 4.3\%$  and  $41.3 \pm 6.2\%$ . The lack of a significant effect observed

with **5k** is likely attributed to the higher variability among replicates.

These observations were also confirmed by confocal microscopy of MitoSOX stained neuron-like cells as shown in Fig. 4C. The cells treated with **5c** and **5p** displayed markedly reduced fluorescence compared to cells treated with MPP + alone and the effect was also stronger than that of EBS. These results demonstrate the dramatic reduction of cellular superoxide by EBS is mediated by quenching of extramitochondrial superoxide radicals. On the other hand compounds **5c** and **5p** are highly effective against both mitochondrial and extramitochondrial superoxide

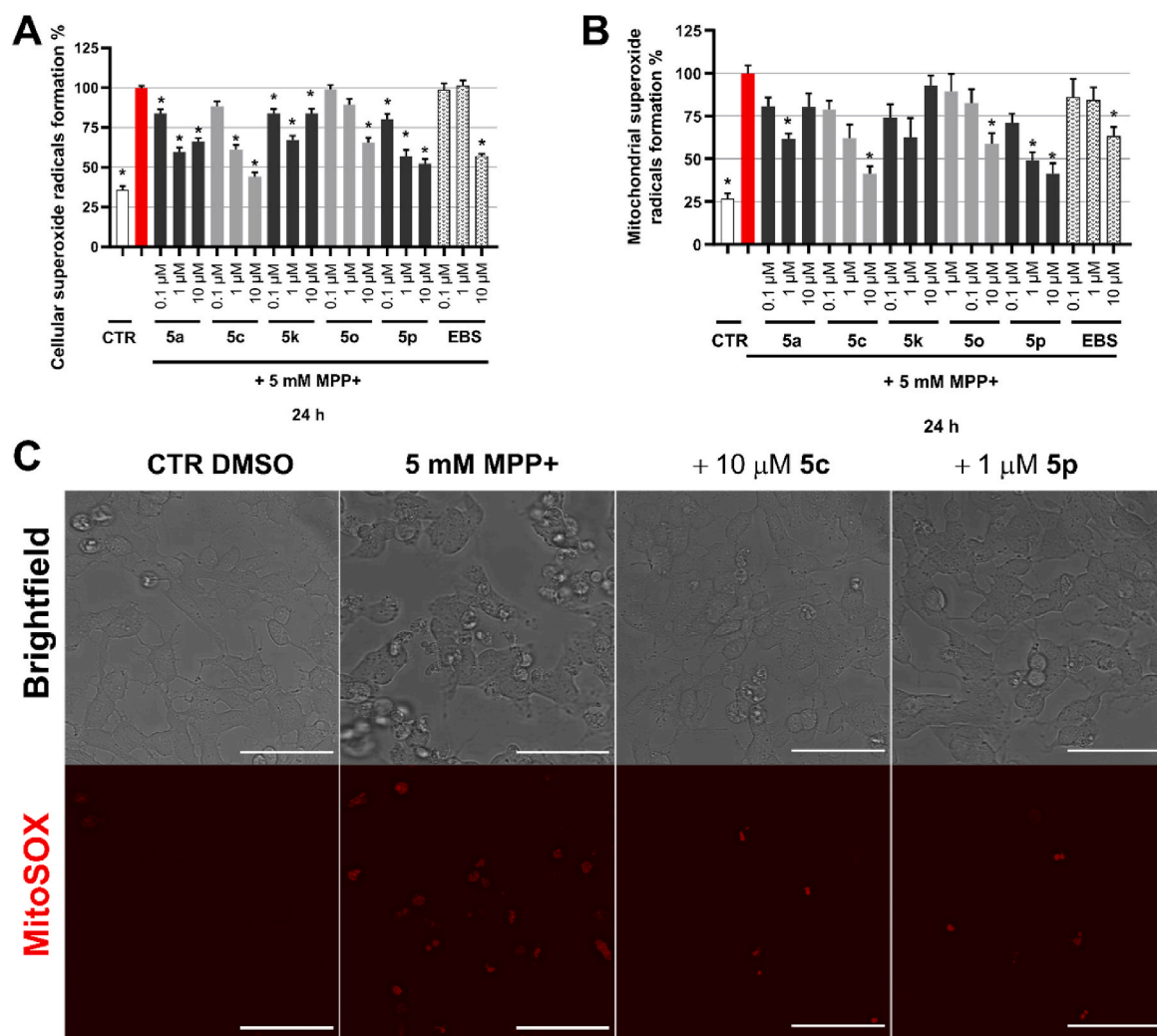


**Fig. 4.** A) MPP + -induced production of cellular superoxide radicals in neuron-like SH-SY5Y cells. B) The activity of derivatives **5a-p** and ebselen on the over-production of mitochondrial superoxide radicals in MPP + -induced model of PD in neuron-like SH-SY5Y cells. Triplicate experiments in at least four independent days. The asterisks designate statistically significant comparisons ( $P < 0.05$ ) with the sample treated with 5 mM MPP+. A value of  $P < 0.05$  was considered statistically significant. C) Representative fluorescence microphotographs of MitoSOX-stained neuron-like SH-SY5Y cells. Bar = 50  $\mu$ m.

radicals.

#### 2.4. Novel quinoline derivatives, but not ebselen maintain mitochondrial membrane potential and decrease phosphorylation of ERK1/2 under stress

Inspired by the results of the measurement of mitochondrial superoxide production, described in the previous sections, we decided to investigate the effect of the compounds on mitochondrial membrane potential (MMP). The cells were co-treated with the toxin and the compounds **5a-5p** or EBS for 2 h. After that, mitochondrial membrane potential was evaluated using JC10 ratiometric assay. MPP + induced depolarization of mitochondria which shifted red/green JC10 signal ratio toward green colour which corresponds to the monomeric form [51]. As shown in Fig. 5A, MPP + caused a dramatic depolarization to  $44.1 \pm 2.2$  % compared to DMSO control (100 %). Notably, while EBS failed to protect mitochondria, all test compounds demonstrated significant MMP restoration. Compounds **5k** and **5o** exhibited particularly high activity. At a concentration of 0.1  $\mu$ M, the signal reached  $78.7 \pm 4.5$  % and  $91.7 \pm 8.3$  % of the control values, respectively. At 1  $\mu$ M, both compounds provided complete protection. Compounds **5a** at 1  $\mu$ M ( $70.6 \pm 3.6$  %), **5c** at 10  $\mu$ M ( $66.8 \pm 3.0$  %) and **5p** at 1  $\mu$ M ( $78.5 \pm 5.6$  %) shown lower but still significant protective activity on MPP. The effect was also confirmed using confocal microscopy of JC10 stained cells

(Fig. 5C).

Finally, we evaluated the activity of selected compound **5c** and EBS at 1–10  $\mu$ M on modulation of Akt and ERK1/2 kinases after the MPP + treatment using western blotting. Akt as key kinase in PI3K/Akt pathway plays important role in survival, proliferation, neuronal development and also cell death [52,53] and ERK1/2 is involved in cell survival, autophagy and related mitophagy [54,55]. Moreover, these signaling pathways are strongly affected by MPP + intoxication [56]. Neuron-like SH-SY5Y were co-treated with 5 mM MPP+ and selected compounds for 24 h with subsequent collection of cells for protein isolation. As shown in Fig. 5B, MPP + increased phosphorylation of both Akt (on Ser473, *p*-Akt) and ERK1/2 compared to control cells. Co-treatment with compounds at 1–10  $\mu$ M yielded interesting results. While the **5c** compound normalized *p*-Akt levels, EBS did not affect the *p*-Akt concentration. Additionally, **5c** also normalized *p*-ERK1/2 levels while the effect of EBS at protective concentration (10  $\mu$ M) was much more limited.

Interestingly *p*-ERK1/2 elevation and downregulation associated with neuroprotective effect was also discussed in study of Park et al., 2022 [56]. Moreover phosphorylation of Akt and ERK1/2 was strongly associated with both impairment of mitochondria and oxidative stress [54,57].

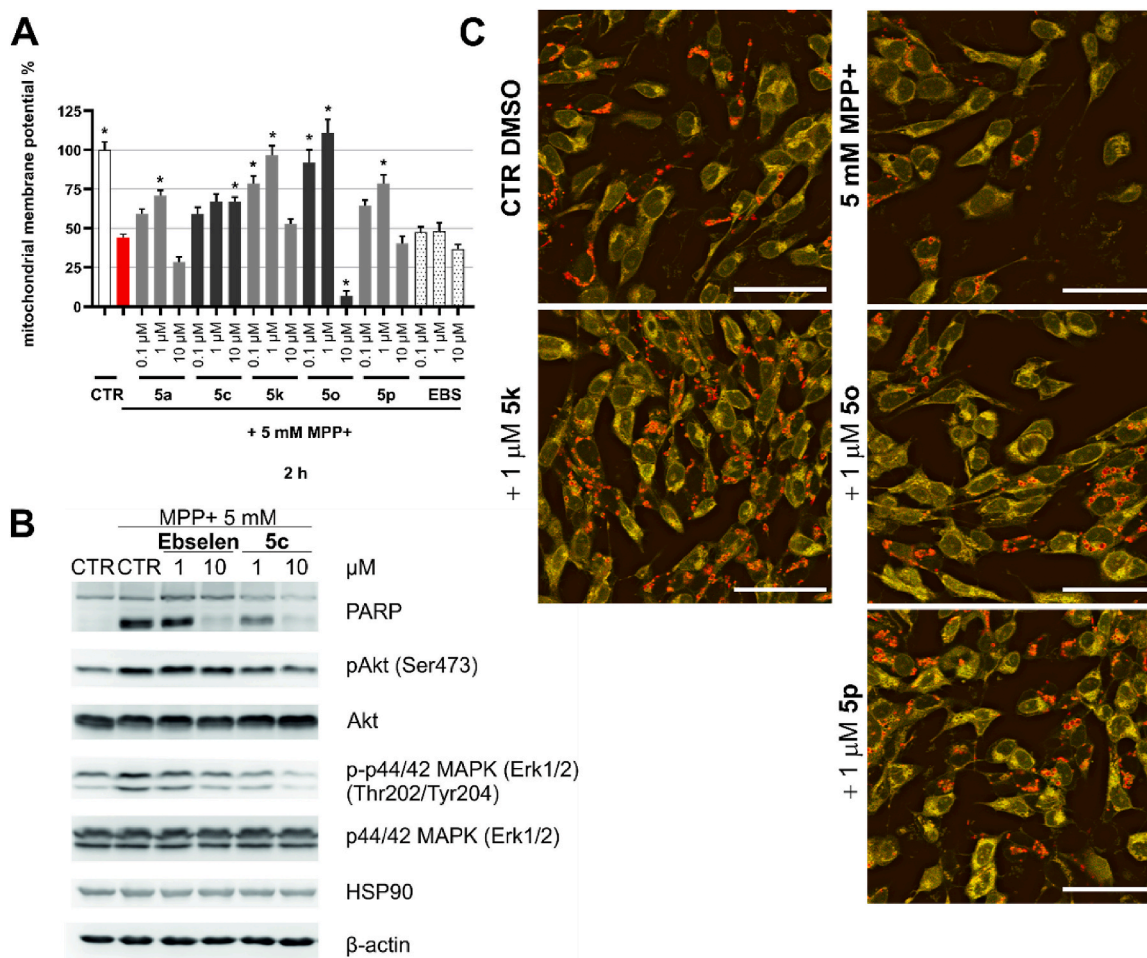


**Fig. 5.** –A) The activity of derivatives **5a** – **5p** and EBS on mitochondrial membrane potential in the MPP + -induced model. Triplicate experiments in three independent days. The asterisks designate statistically significant comparisons ( $P < 0.05$ ) with the sample treated with 5 mM MPP+. B) The effect of compounds **5c** and ebselen on proteins involved in cell death and mitochondria. The cells were co-treated by toxin MPP+ and compounds in selected concentrations (shown as  $\mu\text{M}$ ) for 24 h, lysed and analyzed by immunoblotting. C) Representative fluorescence microphotographs of JC10 stained neuron-like SH-SY5Y co-treated by 5 k-p and 5 mM MPP + effect of compounds **5c-p** and ebselen. Bar = 50  $\mu\text{m}$ .

#### 2.4.1. Inhibition of cholinesterases by novel quinoline derivatives

Despite symptomatic limitations, AChE and BChE inhibition in PD and AD remains therapeutically significant, improving cognition [58], alleviating psychosis [59] and even influencing patient mortality [60].

Based on these evidences and existing quinoline derivatives blocking these enzymes, we tested selected derivatives **5a-p** in AChE and BChE inhibitory tests.

Synthesized derivatives were examined *in vitro* for their potential to inhibit the function of AChE and BChE using modified Ellman's spectrophotometric method. The activities are expressed as  $\text{IC}_{50}$  values, i.e., concentrations leading to 50 % inhibition of enzymatic activity (Table 3). Based on the  $\text{IC}_{50}$  values for AChE and BChE, we calculated

**Table 3**  
Inhibition of AChE and BChE and selectivity indexes.

	$\text{IC}_{50}$ ( $\mu\text{M}$ ) AChE	$\text{IC}_{50}$ ( $\mu\text{M}$ ) BChE	$\text{SI}^a$
<b>5a</b>	$34.04 \pm 0.36$	$19.83 \pm 0.06$	1.72
<b>5c</b>	$47.92 \pm 0.92$	$28.52 \pm 0.40$	1.68
<b>5k</b>	$16.38 \pm 0.03$	$10.44 \pm 0.39$	1.57
<b>5o</b>	$20.03 \pm 0.09$	$19.64 \pm 0.18$	1.02
<b>5p</b>	$26.99 \pm 0.08$	$10.74 \pm 0.11$	2.51
donepezil	$0.0167 \pm 0.00001$	$1.67 \pm 0.03$	0.01
ebselen	$12.70 \pm 0.28$	$12.13 \pm 0.65$	1.05

$\text{IC}_{50}$  values are expressed as the mean  $\pm$  SD ( $n =$  three different experiments).

<sup>a</sup> SI (selectivity index) =  $\text{IC}_{50}(\text{AChE}/\text{IC}_{50}(\text{BChE}))$ .

selectivity indexes (SI) that quantified the selectivity for each cholinesterase. SI is the ratio of  $\text{IC}_{50}$  for AChE/ $\text{IC}_{50}$  for BChE. Values above 1 mean stronger inhibition of BChE. For comparison, the clinically used drug donepezil, a selective inhibitor of AChE, and ebselen, a synthetic organoselenium compound, were employed.

Except for derivative **5o**, which exhibits similar potency against both AChE and BChE, all investigated derivatives are more effective in inhibiting BChE. When comparing  $\text{IC}_{50}$  values for the studied derivatives with those of donepezil, it is evident that they do not reach the same level of activity. However, the activity of **5k** on both enzymes is comparable to EBS. Also, derivative **5p** is comparable to EBS in terms of BChE inhibition efficiency. Inhibitory activity of EBS was in line with other study [61]. A comparison of the activities of unsubstituted derivative (5H-spiro [cyclohexane-1,6'-pyrido [2',1':2,3]imidazo [4,5-c]quinoline], **5a**) with the derivative substituted at carbon 10' (10'-methyl-5H-spiro [cyclohexane-1,6'-pyrido [2',1':2,3]imidazo [4,5-c]quinoline], **5k**) shows that this structural modification leads to an approximately two-fold increase in inhibitory potency against both ChEs. When assessing the inhibitory activity against AChE, substitution with bromine on carbon 9' (9'-bromo-5H-spiro [cyclohexane-1,6'-pyrido [2',1':2,3]imidazo [4,5-c]quinoline], **5o**) also appears to be advantageous. On the other hand, the replacement of cyclohexane in **5a** with methyl groups (6,6-dimethyl-5,6-dihydropyrido [2',1':2,3]imidazo [4,5-c]quinoline, **5c**), results in a decrease in the inhibitory efficiency against both ChEs when compared to **5a**. Furthermore, the replacing

cyclohexane (**5o**) with cyclopentane (**5p**) yields a derivative with slightly lower activity against AChE, but with almost double activity against BChE. Taken together, the measurement of AChE and BChE revealed comparable effect to EBS. Based on study of Du and Xie et al., 2015 showing cholinesterases as active contributor to apoptosis by deoxyribonuclease activity [62], strong anti-apoptotic effect of derivatives **5a-p** and EBS could be explain by the inhibition of cholinesterase in the MPP + -induced model of PD.

#### 2.4.2. Neuroprotection by novel quinoline derivative is dependent on CB2 signaling

ERK1/2 and Akt pathways are regulated by CB1 and CB2 receptor signaling [63–65]. Moreover, quinoline derivatives such as F and D (shown in Fig. 1) demonstrated potent CB2 affinity [34]. The CB2 receptor have gained prominence as a promising target for neuroprotective or potentially anti-inflammatory agents, primarily due to their lack of psychoactive side effects, as previously discussed [28]. Taking into account this evidence, along with the observed disparity in the effects on phosphorylation of ERK1/2 and Akt between derivative **5c** and EBS, despite their similar neuroprotective profiles, we decided to study the impact of CB2 receptor modulation on **5c**-mediated neuroprotection in neuron-like SH-SY5Y that are known to express CB2 receptor.

Cells were co-treated with the MPP+ 5 mM and the compound **5c** in presence of CB2 inverse agonist AM630 or antagonist SR144528 at 0.1, 1 or 10  $\mu$ M for 24 h. Interference of these compounds with CB2 signaling-dependent neuroprotection was demonstrated in previous studies [66–68]. Both CB2 ligands were also tested alone and as a co-treatment with MPP + toxin (Fig. 6). AM630 showed toxic effect only at the highest concentration of 10  $\mu$ M and both compounds potentiated toxic effect of MPP+.

While AM630 by itself caused about 12 % increase in cell death at the highest concentration tested (10  $\mu$ M), no negative effects of SR144528 treatment were observed. Both compounds increased MPP + toxicity only at 10  $\mu$ M. The neuroprotective effect of compound **5c** at either 1  $\mu$ M or 10  $\mu$ M was attenuated in dose-dependent manner by both compounds at their concentrations that did not potentiate MPP + activity.

Taken together, these observations support the hypothesis that **5c**-mediated neuroprotection in MPP + -induced model of PD depends on CB2Rs activation. Evaluation of a direct activation of the CB2 receptor was carried out by cAMP quantification after the treatment of CB2-transfected CHO cells (LeadHunter assay offered by CEREP company). No receptor activation was observed at either 1 or 10  $\mu$ M concentration,

indicating that **5c** acts downstream of CB2R.

#### 2.4.3. Evaluation of interactions with BChE binding site using molecular docking

As shown above, derivatives **5a-p** is similarly potent BChE inhibitors as EBS. In this section we examined interactions of two derivatives **5c**, **5k** and EBS with the catalytic site of human BChE (PDB: 4XII) using the molecular docking. Fig. 7A shows that both EBS and novel derivatives position polar groups (keto group or imidazole nitrogen, respectively) deep in the BChE cavity. In addition, aromatic segments of all derivatives are almost aligned, while aliphatic parts of **5c** and **5k** extend outward from the binding site. Notably, both quinoline derivatives form H-bond of similar length (2.0 Å) with imidazole nitrogen of His438 (Fig. 7B and C). Higher binding energy of **5k** (–11.0 kcal/mol) in comparison to **5c** (–9.8 kcal/mol) can be possibly explained by stronger hydrophobic interactions of cyclohexyl ring in **5k** with Pro285. EBS has lower binding energy than the quinolines (8.6 kcal/mol), however it forms several strong (<2.5 Å) to weaker (>2.5 Å) H-bonds between its keto group and the enzyme's active site (His438–2.1 Å, Ser198–2.9 Å, Gly116–2.8 Å, Gly117–3.2 Å) (see Fig. 7D).

### 3. Conclusion

A novel group of 5,6-dihydropyrido [2',1':2,3]imidazo [4,5-c]quinolines was prepared by microwave-assisted one-pot telescopic approach. The salient features of this one-pot telescopic protocol include the use of green solvent, reduced reaction time, broad substrate scope and use of microwave irradiation. Subsequently, the waste generation is minimized which projects the one-pot telescopic pathway as a suitable methodology for the large-scale synthesis substituted 5,6-dihydropyrido [2',1':2,3]imidazo [4,5-c]quinolines. Owing to the presence of polyheterocycles, this scaffold has various biological activities.

Several derivatives scored in a high-throughput screening for compounds protecting skin cells against oxidative stress. Observed protection of neuron-like cells, SH-SY5Y differentiated with ATRA, in Parkinson's and Huntington's disease models inspired further mechanistic studies of protective activity against damage induced by 1-methyl-4-phenylpyridinium (MPP+), a compound causing Parkinson's disease. In summary, our data demonstrate that the novel compounds exhibit similar or higher potency than ebselen in protecting neuron-like cells against MPP + -induced cell death and total cellular superoxide production. However, they exhibit a significantly higher capacity to reduce mitochondrial superoxide and preserve mitochondrial membrane

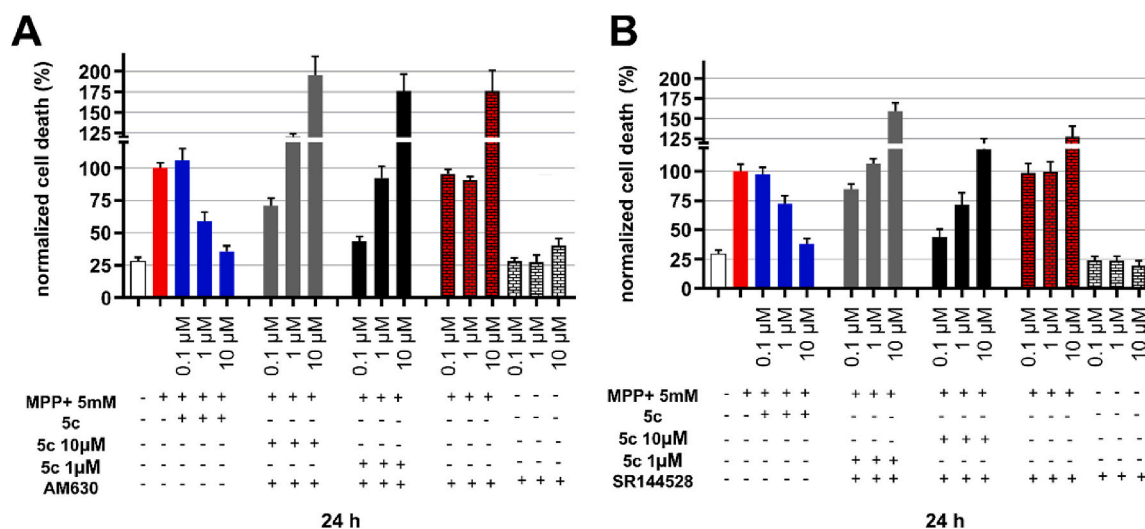
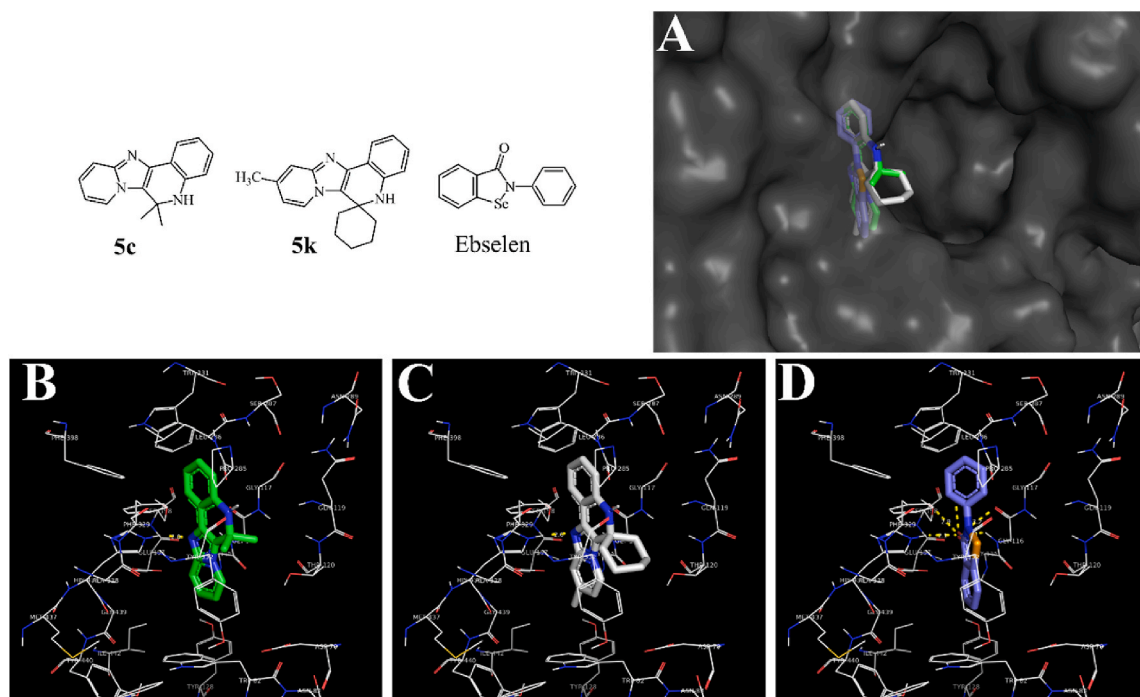


Fig. 6. The effect of cannabinoid receptor 2 inverse agonist AM630 (Panel A) and antagonist SR144528 (Panel B) on neuroprotective effect of **5c** in MPP + induced model of PD on neuron-like SH-SY5Y cells. Triplicate experiments in three independent days.



**Fig. 7.** Structures of **5c**, **5k** and ebselen and their docking into catalytic active site of butyrylcholinesterase (BChE) (PDB:4XII). Compounds in their best poses (A). Amino acid residues interacting with compounds **5c** (green, B), **5k** (grey, C) and ebselen (blue, D).

potential. We also observed marked differences between the compound **5c** and EBS in terms of normalizing MPP + -induced phosphorylation of Akt and ERK1/2. While Akt phosphorylation is generally associated with cell survival [69], under conditions of oxidative stress, it can contribute to cell death [70–73], which we hypothesize is the case in our model. Decreased Akt and ERK1/2 phosphorylation probably reflects protective effects of the novel compounds at the mitochondrial level absent for ebselen. Further studies showed interaction with two established mechanisms relevant for the treatment of neurodegeneration, namely CB2 signaling and acetylcholine metabolism. Compounds with such dual activity can offer both neuroprotection and symptom relief.

## 4. Experimental procedures

### 4.1. Chemistry

#### 4.1.1. Instruments and methods

Unless otherwise indicated, all common reagents and solvents were used as obtained from commercial suppliers without further purification.  $^1\text{H}$  NMR (400 MHz) and  $^{13}\text{C}$  NMR (100 MHz) were recorded on a Bruker DRX400 spectrometer. Chemical shifts are reported in ppm relative to the internal solvent peak. Coupling constants,  $J$ , are given in Hz. Multiplicities of peaks are given as: d (doublet), m (multiplet), s (singlet), and t (triplet). Mass spectra were recorded on a PerkinElmer Clarus 600 GC-MS spectrometer. HRMS were recorded on LC-QTOF-HRMS. IR spectra were recorded on a Bomem DA8 3FTS spectrometer. Microwave-assisted reactions were carried out in a Catalyst Scientific Microwave oven system (Model No: CATA R (Catalyst System, Pune) operating at 2450 MHz equipped with glass vial extension by a condenser was used for performing the reaction. The microwave was equipped with a temperature control system (external probe). All the starting materials, such as substituted 2-aminopyridine, 2-Bromo-2-nitroacetophenone, and substituted ketones were purchased from either Sigma-Aldrich or Avra scientific limited.

#### 4.1.2. Procedure for the sequential synthesis of 5'H-spiro [cyclohexane-1,6'-pyrido [2,1:2,3]imidazo [4,5-c]quinoline] **5a**

To a round bottom flask, 2-aminopyridine **1a** (0.150 g, 1.6 mmol, 1.0 equiv.) and 2-bromo-2-nitro acetophenone **2** (0.408 g, 1.6 mmol, 1.0 equiv.) were charred using 5 mL of  $\text{H}_2\text{O}$ :IPA (1:3) solvent and the resultant mixture was irradiated for 8 min at 75 °C. The progress of the reaction was monitored by TLC. After completion of the reaction, conc HCl (0.045 g, 1.26 mmol, 1.5 equiv) is added to the mixture followed by zinc dust (0.163 g, 2.4 mmol, 3.0 equiv) under vigorous stirring. The resulting reaction mixture was irradiated 70 °C under microwave for 5 min. After completion of the reaction as monitored by TLC, Zn dust was removed by centrifugation, then cyclohexanone **4a** (0.102 g, 0.96 mmol, 1.1 equiv.) along with trifluoroacetic acid (0.107 g, 0.9 mmol, 1.0 equiv.) were added. The same reaction mixture was irradiated at 280 W for 10 min at 70 °C. Progress of the reaction was monitored by TLC. After completion of the reaction, solvent was removed using rotary evaporator and the resulting reaction mixture was neutralised with saturated sodium bicarbonate solution. Then, it is extracted with ethyl acetate (10 mL thrice) and all the fractions of the organic layer were combined and dried over sodium sulfate. The combined filtrate was then evaporated to obtain crude extracts. The combined extracts were triaturated with 10 % EA in hexane to obtain 5'H-spiro [cyclohexane-1,6'-pyrido [2',1':2,3]imidazo [4,5-c]quinoline] **5a**.

Yield = 93 %; white solid;  $R_f$  = 0.60 (40%EtOAc/*n*-hexane);  $^1\text{H}$  NMR (400 MHz,  $\text{DMSO}-d_6$ )  $\delta$  8.97 (d,  $J$  = 6.96 Hz, 1H), 7.89 (d,  $J$  = 8.92 Hz, 1H), 7.74 (t,  $J$  = 8.64 Hz, 1H), 7.53 (d,  $J$  = 6.44 Hz, 1H), 7.32 (t,  $J$  = 6.76 Hz, 1H), 7.09 (t,  $J$  = 7.04 Hz, 1H), 7.00 (d,  $J$  = 7.84 Hz, 1H), 6.62 (t,  $J$  = 7.04 Hz, 1H), 6.53 (s, 1H), 2.33–2.25 (m, 2H), 2.01–1.98 (m, 2H), 1.90–1.83 (m, 2H), 1.71–1.68 (m, 1H), 1.61–1.58 (m, 3H);  $^{13}\text{C}$  NMR (100 MHz,  $\text{DMSO}-d_6$ )  $\delta$  143.7, 143.4, 133.3, 130.4, 128.5, 127.3, 122.4, 121.8, 116.6, 115.3, 115.1, 114.1, 111.7, 56.1, 34.8, 24.3, 19.7; HRMS (ESI,  $m/z$ ) calcd for  $\text{C}_{19}\text{H}_{20}\text{N}_3$ ;  $m/z$  290.1657; Found: 290.1669 (M + H); IR ( $\text{cm}^{-1}$ , KBr): 3331, 2929, 1660, 1423, 1330, 736.

## 4.2. Biological evaluation

### 4.2.1. Drugs and reagents

Dulbecco's Modified Eagle Medium/Nutrient Mixture F-12 (DMEM/F-12), penicillin, streptomycin, fetal bovine serum, trypsin, all-trans retinoic acid, propidium iodide, dihydroethidium, *N*-acetylcysteine, ebselen, 3-nitropropionic acid, MPP + iodide, AM630, SR144528, buffer components for One-step caspase 3,7 assay, the mitochondrial membrane JC10 kit, caspase-3,7 substrate (Ac-DEVD-AFC), LDH release assay kit, acetylcholinesterase, butyrylcholinesterase, acetylthiocholine and butyrylthiocholine were purchased from Merck. The YOPRO-1 and MitoSOX kit was obtained from ThermoFisher.

### 4.2.2. Antibodies

PARP (46D11) Rabbit mAb #9532 Cell Signaling.  
Phospho-Akt (Ser473) (D9E) XP® Rabbit mAb #4060 Cell Signaling.  
Phospho-p44/42 MAPK (Erk1/2) (Thr202/Tyr204) antibody #9101 Cell Signaling.  
HSP90 (C45G5) Rabbit mAb #4877 Cell Signaling.  
Akt (pan) (C67E7) Rabbit mAb #4691 Cell Signaling  
p44/42 MAPK (Erk1/2) antibody #9102 Cell Signaling  
anti- $\beta$ -actin (C4): sc-47778 Santa Cruz Biotechnology  
anti-rabbit IgG, HRP-linked antibody #7074 Cell Signaling  
anti-mouse IgG (whole molecule)-peroxidase antibody A9044 Merck.

### 4.2.3. AChE and BChE inhibition studies

The inhibitory activity of investigated derivatives for AChE (obtained from electric eel) and BChE (obtained from equine serum) was determined spectrophotometrically using modified Ellman's method to quantify them in terms of IC<sub>50</sub> values. The enzyme activity in the final reaction mixture (2000  $\mu$ L) was 0.2 U/mL, the concentration of acetylthiocholine (ATCh) or butyrylthiocholine (BTCh) was 40  $\mu$ M, and the concentration of DTNB was 100  $\mu$ M for all reactions. The investigated derivatives were dissolved in DMSO and then diluted with demineralized water (conductivity 3  $\mu$ S, equipment supplier BKG Water Treatment, Hradec Králové, Czech Republic) as required. Five different inhibitor concentrations were used for all tested compounds in the final reaction mixture. All experiments were performed in triplicate. The average values of the reaction rate ( $v_0$  - uninhibited reaction,  $v_i$  - inhibited reaction) were used to construct the dependence of  $v_0/v_i$  on the concentration of inhibitors. IC<sub>50</sub> values were calculated from the obtained regression curve equations.

### 4.2.4. SH-SY5Y cell culture and differentiation

The SH-SY5Y cell line (European Collection of Authenticated Cell Cultures) was cultivated in DMEM/F-12 Ham's Nutrient mix (1:1) in a humidified CO<sub>2</sub> incubator at 37 °C. Cells were passaged two or three times a week by trypsin and were used in passage under 20. For biological evaluation, SH-SY5Y cells were used in differentiated (neuron-like) phenotype as shown in previous works [74].

### 4.2.5. Cell treatment, cytotoxicity and neuroprotective activity evaluation

Tested compounds and positive controls were prepared as DMSO solutions. Neuron-like SH-SY5Y cells were used at density 20 000 cells per well of 96-well plate for all assays. Cytotoxicity was evaluated as described in Ref. [41]. Briefly, Neuron-like SH-SY5Y cells were treated by the compounds to final concentrations 0.1, 1 and 10  $\mu$ M or higher (positive controls) and incubated for 72 h. Control cells were then treated with 1 % Triton X-100 for 1 min causing death of all cells. Subsequently all cells were stained with propidium iodide and fluorescence was measured according to Ref. [74]. Proportion of death cells was expressed relative to the Triton-X-100-treated control group. For neuroprotective activity in the 3-NPA model we used the protocol shown in Ref. [41] and similar procedure was also used in the MPP + -model. DMSO concentration did not exceed 0.5 %. The effect of compounds was measured PI

as shown above. The activity of promising compounds was validated using a commercial LDH release kit (Merck) according to manufacturer's protocol.

### 4.2.6. Measurement of oxidative stress by dihydroethidium (DHE) and MitoSOX assays

For MPP + model, dihydroethidium (DHE) [74] and MitoSOX assays were used for quantification of cellular and mitochondrial superoxide radical formation. First, DHE assay was performed as previously described [74]. Briefly, neuron-like SH-SY5Y cells were co-treated with protective **compounds 5a-p** or **EBS** and with 5 mM MPP + for 24 h. After the incubation, the plates were centrifuged at 500 $\times$ g, growth medium was replaced with 10  $\mu$ M DHE in PBS for 30 min, and fluorescence at 500/580 nm (ex./em.) was measured by Infinite M200 Pro microplate reader (Tecan, Austria). Second, MitoSOX assay was performed according to manufacturer's protocol. Plates with neuron-like SH-SY5Y cells were centrifuged, growth medium was replaced by 5  $\mu$ M MitoSOX in HBSS buffer. After the 30 min incubation in 37 °C, fluorescence was measured 500/580 nm (ex./em.) by Infinite M200 Pro microplate reader (Tecan, Austria). For fluorescence microscopy, 50 000 cells were seeded to  $\mu$ -Slide 8 (IBIDI) slides, differentiated by ATRA and then co-treated by 5 mM MPP+ and the compounds. After 24 h, the cells were stained with MitoSOX solution and observed under Leica SP2 confocal laser-scanning microscope (63 $\times$  objective). Images were processed in ImageJ software (Fiji).

### 4.2.7. Measurement of apoptosis (YOPRO1 and caspase 3/7 activity)

Induction of apoptosis in MPP + model in neuron-like SH-SY5Y cells was evaluated by YO-PRO1 staining according to Ref. [75]. YO-PRO1 dye enters cells in the early stage of apoptosis, intercalates with DNA and produces green fluorescence. Briefly, neuron-like SH-SY5Y cells were seeded in 96-well plates and differentiated as described above. After the co-treatment with **5a-p** and MPP + for 24 h, the plates were centrifuged at 500 $\times$ g, medium was replaced by 1  $\mu$ M YO-PRO1 solution in PBS and cells were kept at laboratory temperature for 15 min. Resulting fluorescence was measured at 488/530 nm (ex./em.) using Infinite M200 Pro microplate reader (Tecan, Austria). Slides for microscopy were prepared as described for MitoSOX assay above, stained with YO-PRO1 and observed under Leica SP2 confocal laser-scanning microscope (63 $\times$  objective). Images were processed in ImageJ software (Fiji).

Apoptosis induction after 24 h cotreatment with the compounds and MPP+ was also measured by the orthogonal caspase-3/7 activation assay described by Carrasco et al., 2003 [76] with modification according to Ref. [41].

### 4.2.8. Measurement of mitochondrial membrane potential by JC10 assay

Mitochondrial membrane potential in neuron-like SH-SY5Y cells was measured after 2 h of exposure to MPP+ and the test compounds using JC10 assay according to manufacturer protocol as also described in Ref. [41]. For live imaging, 50 000 cells/well were seeded in  $\mu$ -Slide 8 (IBIDI) slides, differentiated and treated with the compounds and MPP+. After 2 h, cells were stained by JC10 according to manufacturer's protocol and scanned using Leica SP2 confocal laser-scanning microscope (63 $\times$  objective). Images were processed in ImageJ software (Fiji).

### 4.2.9. Electrophoresis and western blotting

After the treatment, cells were harvested and lysed in RIPA buffer. Proteins were separated by sodium dodecyl-sulfate polyacrylamide gel electrophoresis (SDS-PAGE) and transferred to nitrocellulose membranes as described in Ref. [77]. Western blotting was done according to the published procedure [78]. Proteins were detected using primary antibodies: *anti*-PARP #9532 (full-length PARP-1 and the large fragment), *anti*-phospho-Akt #4060, *anti*-Akt #4691, *anti*-phospho-p44/42 MAPK #9101, *anti*-p44/42 MAPK #9102 and *anti*-HSP90 #4877 from Cell Signaling Technology, Danvers, Massachusetts, USA and

anti- $\beta$ -actin (C4 sc-47778) from Santa Cruz Biotechnology (Dallas, Texas, USA). Secondary HRP-conjugated anti-rabbit and anti-mouse IgG antibody were from Cell Signaling Technology, Danvers, Massachusetts, USA and from Merck, Darmstadt, Germany, respectively. HSP90 and  $\beta$ -actin were used as loading controls. After the incubation with **Enhanced Chemiluminescence substrate** HRP substrate (Pierce), chemiluminescence was scanned by a CCD camera. The experiment was performed three times.

#### 4.2.10. Molecular docking study

All 3D structures of compounds **5c**, **5k**, ebselen and WIN55,212–2 were prepared in Molecular Operating Environment 2010.12 (Chemical computing group, Montreal, Canada). To each compounds, polar hydrogens were added. Energy minimization based on MMFF94x force field (gradient 0.001) was performed. Crystal structures of human BChE (PDB: 4xii) was prepared by water and solvents removal and addition of hydrogens. Both ligands and proteins were pre-processed by AutoDock Tools program [79] and docking was performed in AutoDock Vina 1.05 [80]. Resulting figures were created using Pymol ver.2.6.0a0 (Schrodinger, LLC).

#### 4.2.11. Statistical analysis

Data displayed as bar graphs were analyzed in GraphPad Prism 9.3.1 (GraphPad software, La Jolla, CA, USA). Normality was evaluated by Levene's test. Analysis of variance (ANOVA) with Tukey multiple comparison test (normal distribution: Figs. 3A and 4A) and non-parametric Kruskal-Wallis test followed by post-hoc Mann-Whitney test with Bonferroni p-value correction (non-normal distribution; Fig. 3B, C, 4B, 5A) were performed using PAST software (version 1.97) [81]. P-value <0.05 was considered statistically significant.

#### CRedit authorship contribution statement

**Sushovan Jena:** Writing – review & editing, Writing – original draft, Investigation. **Gabriel Gonzalez:** Writing – review & editing, Writing – original draft, Supervision, Investigation, Conceptualization. **Dominik Vitek:** Writing – review & editing, Investigation. **Marie Kvasnicová:** Writing – review & editing, Investigation. **Šárka Štěpánková:** Writing – review & editing, Investigation. **Miroslav Strnad:** Writing – review & editing, Resources. **Jirí Voller:** Writing – review & editing, Writing – original draft, Supervision, Investigation, Conceptualization. **Kaushik Chanda:** Writing – review & editing, Writing – original draft, Supervision, Investigation, Conceptualization.

#### Declaration of competing interest

The authors declare that they have no known competing financial interests or personal relationships that could have appeared to influence the work reported in this paper.

#### Data availability

Data will be made available on request.

#### Acknowledgment

The project was supported by project LX22NPO5107 (MEYS) financed by EU – Next Generation EU, project CZ-OPENSREEN (LM2023052) financed by Czech Ministry of Education, Health and Sports and by a grant of the Czech Science Foundation No. 23-05389S. Authors would like to thank Mrs. Dita Jordová for excellent technical support. KC thanks Vice Chancellor of Rabindranath Tagore University, Hojai for his keen interest in this work.

## Appendix A. Supplementary data

Supplementary data to this article can be found online at <https://doi.org/10.1016/j.ejmech.2024.116592>.

## References

- [1] J.C. Bridi, F. Hirth, Mechanisms of  $\alpha$ -synuclein induced synaptopathy in Parkinson's disease, *Front. Neurosci.* 12 (2018) 80, <https://doi.org/10.3389/fnins.2018.00080>.
- [2] T. Moors, S. Paciotti, D. Chiasserini, P. Calabresi, L. Parnetti, T. Beccari, W.D. van de Berg, Lysosomal dysfunction and  $\alpha$ -synuclein aggregation in Parkinson's disease: diagnostic links, *Mov. Disord.* 31 (2016) 791–801, <https://doi.org/10.1002/mds.26562>.
- [3] Z. Wei, X. Li, X. Li, Q. Liu, Y. Cheng, Oxidative stress in Parkinson's disease: a systematic review and meta-analysis, *Front. Mol. Neurosci.* 11 (2018) 236, <https://doi.org/10.3389/fnmol.2018.00236>.
- [4] H.E. Moon, S.H. Paek, Mitochondrial dysfunction in Parkinson's disease, *Exp. Neurobiol.* 24 (2015) 103–116, <https://doi.org/10.5607/en.2015.24.2.103>.
- [5] Q. Wang, Y. Liu, J. Zhou, Neuroinflammation in Parkinson's disease and its potential as therapeutic target, *Transl. Neurodegener.* 4 (2015) 19, <https://doi.org/10.1186/s40035-015-0042-0>.
- [6] U.K. Rinne, Problems associated with long-term levodopa treatment of Parkinson's disease, *Acta Neurol. Scand. Suppl.* 95 (1983) 19–26, <https://doi.org/10.1111/j.1600-0404.1983.tb01513.x>.
- [7] M.W. Hayes, V.S. Fung, T.E. Kimber, J.D. O'Sullivan, Updates and advances in the treatment of Parkinson disease, *Med. J. Aust.* 211 (2019) 277–283, <https://doi.org/10.5694/mja2.50224>.
- [8] M. Carbone, S. Duty, M. Rattray, Riluzole neuroprotection in a Parkinson's disease model involves suppression of reactive astrocytosis but not GLT-1 regulation, *BMC Neurosci.* 13 (2012), <https://doi.org/10.1186/1471-2202-13-38>, 38–38.
- [9] A.H. Schapira, C.W. Olanow, Neuroprotection in Parkinson disease: mysteries, myths, and misconceptions, *JAMA* 291 (2004) 358–364, <https://doi.org/10.1001/jama.291.3.358>.
- [10] E. Arias, S. Gallego-Sandín, M. Villarroya, A.G. García, M.G. López, Unequal neuroprotection afforded by the acetylcholinesterase inhibitors galantamine, donepezil, and rivastigmine in SH-SY5Y neuroblastoma cells: role of nicotinic receptors, *J. Pharmacol. Exp. Therapeut.* 315 (2005) 1346–1353, <https://doi.org/10.1124/jpet.105.090365>.
- [11] J.R. Das, Y. Tizabi, Additive protective effects of donepezil and nicotine against salsolinol-induced cytotoxicity in SH-SY5Y cells, *Neurotox. Res.* 16 (2009) 194–204, <https://doi.org/10.1007/s12640-009-9040-2>.
- [12] Y. Tian, Y. He, W. Song, E. Zhang, X. Xia, Neuroprotective effect of deferoxamine on N-methyl-D-aspartate-induced excitotoxicity in RGC-5 cells, *Acta Biochim. Biophys. Sin.* 49 (2017) 827–834, <https://doi.org/10.1093/abbs/gmx082>.
- [13] P. Jenner, Preclinical evidence for neuroprotection with monoamine oxidase-B inhibitors in Parkinson's disease, *Neurology* 63 (2004) S13–S22, [https://doi.org/10.1212/wnl.63.7\\_suppl\\_2.s13](https://doi.org/10.1212/wnl.63.7_suppl_2.s13).
- [14] C.W. Olanow, A rationale for dopamine agonists as primary therapy for Parkinson's disease, *Can. J. Neurol. Sci.* 19 (2015) 108–112, <https://doi.org/10.1017/S0317167100041469>.
- [15] N. Giladi, M.P. McDermott, S. Fahn, S. Przedborski, J. Jankovic, M. Stern, C. Tanner, Freezing of gait in PD: prospective assessment in the DATATOP cohort, *Neurology* 56 (2001) 1712–1721, <https://doi.org/10.1212/wnl.56.12.1712>.
- [16] W. Poewe, K. Seppi, K. Marini, P. Mahlknecht, New hopes for disease modification in Parkinson's Disease, *Neuropharmacology* 171 (2020) 108085, <https://doi.org/10.1016/j.neuropharm.2020.108085>.
- [17] M. Solayman, M.A. Islam, F. Alam, M.I. Khalil, M.A. Kamal, S.H. Gan, Natural products combating neurodegeneration: Parkinson's disease, *Curr. Drug Metabol.* 18 (2017) 50–61, <https://doi.org/10.2174/1389200217666160709204826>.
- [18] T. van Laar, P.P. De Deyn, D. Aarsland, P. Barone, J.E. Galvin, Effects of cholinesterase inhibitors in Parkinson's disease dementia: a review of clinical data, *CNS neurosci. Therapy* 17 (2011) 428–441, <https://doi.org/10.1111/j.1755-5949.2010.00166.x>.
- [19] S. Onder, L.M. Schopfer, W. Jiang, O. Tacal, O. Lockridge, Butyrylcholinesterase in SH-SY5Y human neuroblastoma cells, *Neurotoxicology* 90 (2022) 1–9, <https://doi.org/10.1016/j.neuro.2022.02.006>.
- [20] M. Scheiner, M. Hoffmann, F. He, E. Poeta, A. Chatonnet, B. Monti, T. Maurice, M. Decker, Selective pseudo-irreversible butyrylcholinesterase inhibitors transferring antioxidant moieties to the enzyme show pronounced neuroprotective efficacy in vitro and in vivo in an Alzheimer's disease mouse model, *J. Med. Chem.* 64 (2021) 9302–9320, <https://doi.org/10.1021/acs.jmedchem.1c00534>.
- [21] U. Kosak, B. Brus, D. Knez, R. Sink, S. Zakej, J. Trontelj, A. Pišlar, J. Šlenc, M. Gobec, M. Živin, L. Tratnjek, M. Perše, K. Salat, A. Podkova, B. Filipek, F. Nachon, X. Brazzolotto, A. Więckowska, B. Malawska, J. Stojan, I.M. Raščan, J. Kos, N. Coquelle, J.-P. Colletier, S. Gobec, Development of an in-vivo active reversible butyrylcholinesterase inhibitor, *Sci. Rep.* 6 (2016) 39495, <https://doi.org/10.1038/srep39495>.
- [22] Q. Li, B. Xiong, Y. Wang, W. Lyu, S. Xing, Y. Chen, Q. Liao, S. He, F. Feng, W. Liu, Y. Chen, H. Sun, A highly effective and stable butyrylcholinesterase inhibitor with multi-faceted neuroprotection and cognition improvement, *Eur. J. Med. Chem.* 239 (2022) 114510, <https://doi.org/10.1016/j.ejmech.2022.114510>.
- [23] S. Darvesh, M.K. Cash, G.A. Reid, E. Martin, A. Mitnitski, C. Geula, Butyrylcholinesterase is associated with  $\beta$ -amyloid plaques in the transgenic

- APPSWE/PSEN1dE9 mouse model of Alzheimer disease, *J. Neuropathol. Exp. Neurol.* 71 (2012) 2–14, <https://doi.org/10.1097/NEN.0b013e31823cc7a6>.
- [24] M. Pohanka, Inhibitors of acetylcholinesterase and butyrylcholinesterase meet immunity, *Int. J. Mol. Sci.* 15 (2014) 9809–9825, <https://doi.org/10.3390/ijms15069809>.
- [25] N.H. Greig, T. Utsuki, D.K. Ingram, Y. Wang, G. Pepeu, C. Scali, Q.-S. Yu, J. Mamczarz, H.W. Holloway, T. Giordano, D. Chen, K. Furukawa, K. Sambamurti, A. Brossi, D.K. Lahiri, Selective butyrylcholinesterase inhibition elevates brain acetylcholine, augments learning and lowers Alzheimer beta-amyloid peptide in rodent, *Proc. Natl. Acad. Sci. U.S.A.* 102 (2005) 17213–17218, <https://doi.org/10.1073/pnas.0508575102>.
- [26] P.T. Francis, A. Nordberg, S.E. Arnold, A preclinical view of cholinesterase inhibitors in neuroprotection: do they provide more than symptomatic benefits in Alzheimer's disease? *Trends Pharmacol. Sci.* 26 (2005) 104–111, <https://doi.org/10.1016/j.tips.2004.12.010>.
- [27] G. Navarro, P. Morales, C. Rodríguez-Cueto, J. Fernández-Ruiz, N. Jagerovic, R. Franco, Targeting cannabinoid CB2 receptors in the central nervous system. Medicinal chemistry approaches with focus on neurodegenerative disorders, *Front. Neurosci.* 10 (2016), <https://doi.org/10.3389/fnins.2016.00406>.
- [28] S.V. More, D.-K. Choi, Promising cannabinoid-based therapies for Parkinson's disease: motor symptoms to neuroprotection, *Mol. Neurodegener.* 10 (2015) 17, <https://doi.org/10.1186/s13024-015-0012-0>.
- [29] S.-Q. Chen, Z.-S. Wang, Y.-X. Ma, W. Zhang, J.-L. Lu, Y.-R. Liang, X.-Q. Zheng, Neuroprotective effects and mechanisms of tea bioactive components in neurodegenerative diseases, *Molecules* 23 (2018) 512, <https://doi.org/10.3390/molecules23030512>.
- [30] M. Alghazwi, Y.Q. Kan, W. Zhang, W.P. Gai, X.X. Yan, Neuroprotective activities of marine natural products from marine sponges, *Curr. Med. Chem.* 23 (2016) 360–382, <https://doi.org/10.2174/0929867323666151127201249>.
- [31] B. Selvaraj, D. Woon Kim, J.S. Park, H. Cheol Kwon, H. Lee, K.Y. Yoo, J. Wook Lee, Neuroprotective effects of 2-heptyl-3-hydroxy-4-quinolone in HT22 mouse hippocampal neuronal cells, *Bioorg. Med. Chem. Lett.* 49 (2021) 128312, <https://doi.org/10.1016/j.bmcl.2021.128312>.
- [32] P. Desos, J.M. Lepagnol, P. Morain, P. Lestage, A.A. Cordi, Structure–Activity relationships in a series of 2(1H)-Quinolones bearing different acidic function in the 3-position: 6,7-dichloro-2(1H)-oxoquinoline-3-phosphonic acid, a new potent and selective AMPA/kainate antagonist with neuroprotective properties, *J. Med. Chem.* 39 (1996) 197–206, <https://doi.org/10.1021/jm950323j>.
- [33] C. Chiruta, D. Schubert, R. Dargusch, P. Maher, Chemical modification of the multitarget neuroprotective compound fisetin, *J. Med. Chem.* 55 (2012) 378–389, <https://doi.org/10.1021/jm2012563>.
- [34] E. Stern, G.G. Muccioli, R. Millet, J.-F. Goossens, A. Farce, P. Chavatte, J. H. Poupaert, D.M. Lambert, P. Depreux, J.-P. Hélichart, Novel 4-Oxo-1,4-dihydroquinoline-3-carboxamide derivatives as new CB2 cannabinoid receptors agonists: synthesis, pharmacological properties and molecular modeling, *J. Med. Chem.* 49 (2006) 70–79, <https://doi.org/10.1021/jm050467q>.
- [35] I. Tomassoli, L. Ismaili, M. Pudlo, C. de Los Ríos, E. Soriano, I. Colmena, L. Gandia, L. Rivas, A. Samadi, J. Marco-Contelles, B. Refouvelet, Synthesis, biological assessment and molecular modeling of new dihydroquinoline-3-carboxamides and dihydroquinoline-3-carbohydrazide derivatives as cholinesterase inhibitors, and Ca channel antagonists, *Eur. J. Med. Chem.* 46 (2011) 1–10, <https://doi.org/10.1016/j.ejmech.2010.08.054>.
- [36] H. Iwamura, H. Suzuki, Y. Ueda, T. Kaya, T. Inaba, *In vitro* and *in vivo* pharmacological characterization of JTE-907, a novel selective ligand for cannabinoid CB2 receptor, *J. Pharmacol. Exp. Therapeut.* 296 (2001) 420–425.
- [37] S. Das, K. Chanda, One-pot telescopic approach to synthesize disubstituted benzimidazoles in deep eutectic solvent, *Synthesis* 56 (2024) 693–699.
- [38] R.N. Rao, S. Das, K. Jacob, M.M. Alam, M.M. Balamuali, K. Chanda, Synthetic access to diverse thiazetidines via a one-pot microwave assisted telescopic approach and their interaction with biomolecules, *Org. Biomol. Chem.* 22 (2024) 3249–3261.
- [39] R.N. Rao, K. Chanda, An expeditious microwave assisted one-pot sequential route to pyridio fused imidazo[4,5-c] quinolines in green media, *New J. Chem.* 45 (2021) 3280–3289.
- [40] Final product **5f** was crystallized by slow evaporation of a solution of ethyl acetate–hexane (1:1, v/v) at room temperature. Crystal data:  $C_{22}H_{22}F_3N_3O_2$ ,  $M = 417.43$  Triclinic, space group P1, The crystal data has been deposited at Cambridge Crystallographic Data Centre [CCDC No. 2330777]. Copies of the data can be obtained free of charge via a [www.ccdc.cam.ac.uk/data\\_request/cif](http://www.ccdc.cam.ac.uk/data_request/cif).
- [41] G. Gonzalez, M. Kvasnica, K. Svrčková, Š. Štěpánková, J.R.C. Santos, M. Perina, R. Jorda, S.M.M. Lopes, T.M.V.D. Pinho e Melo, Ring-fused  $\beta$ -acetoxyandrost-5-enes as novel neuroprotective agents with cholinesterase inhibitory properties, *J. Steroid Biochem. Mol. Biol.* 225 (2023) 106194, <https://doi.org/10.1016/j.jsmb.2022.106194>.
- [42] A.D. Landgraf, A.S. Alseghiani, S. Alaql, S. Thanna, Z.A. Shah, S.J. Sucheck, Neuroprotective and anti-neuroinflammatory properties of ebselen derivatives and their potential to inhibit neurodegeneration, *ACS Chem. Neurosci.* 11 (2020) 3008–3016, <https://doi.org/10.1021/acscchemneuro.0c00328>.
- [43] S. Moussaoui, M.C. Obinu, N. Daniel, M. Reibaud, B. Veronique, A. Imperato, The antioxidant ebselen prevents neurotoxicity and clinical symptoms in a primate model of Parkinson's disease, *Exp. Neurol.* 166 (2001) 235–245, <https://doi.org/10.1006/exnr.2000.7516>.
- [44] P. Risigione, L. Leggio, S.A.M. Cubisino, S. Reina, G. Paternò, B. Marchetti, High-resolution respirometry reveals MPP(+)-mitochondrial toxicity mechanism in a cellular model of Parkinson's disease, *Int. J. Mol. Sci.* 21 (2020), <https://doi.org/10.3390/ijms21217809>.
- [45] K. Ito, Y. Eguchi, Y. Imagawa, S. Akai, H. Mochizuki, Y. Tsujimoto, MPP+ induces necrostatin-1- and ferrostatin-1-sensitive necrotic death of neuronal SH-SY5Y cells, *Cell Death Dis.* 3 (2017) 17013, <https://doi.org/10.1038/cddiscovery.2017.13>.
- [46] S.J. Choi, A. Panhelainen, Y. Schmitz, K.E. Larsen, E. Kanter, M. Wu, D. Sulzer, E. V. Mosharov, Changes in neuronal dopamine homeostasis following 1-methyl-4-phenylpyridinium (MPP+) exposure, *J. Biol. Chem.* 290 (2015) 6799–6809, <https://doi.org/10.1074/jbc.M114.631556>.
- [47] H. Xicoy, B. Wieringa, G.J.M. Martens, The SH-SY5Y cell line in Parkinson's disease research: a systematic review, *Mol. Neurodegener.* 12 (2017) 10, <https://doi.org/10.1186/s13024-017-0149-0>.
- [48] W. Qi, D. Zeng, X. Xiong, Q. Hu, Knockdown of SEMA7A alleviates MPP+–induced apoptosis and inflammation in BV2 microglia via PPAR- $\gamma$  activation and MAPK inactivation, *Immunity, Inflammation and Disease* 11 (2023) e756, <https://doi.org/10.1002/iid3.756>.
- [49] M. Ramalingam, S.-j. Kim, The neuroprotective role of insulin against MPP+–Induced Parkinson's disease in differentiated SH-SY5Y cells, *J. Cell. Biochem.* 117 (2016), <https://doi.org/10.1002/jcb.25376>.
- [50] W.M. Zawada, G.P. Banninger, J. Thornton, B. Marriott, D. Cantu, A. L. Rachubinski, M. Das, W.S. Griffin, K.E. Jones, Generation of reactive oxygen species in 1-methyl-4-phenylpyridinium (MPP+) treated dopaminergic neurons occurs as an NADPH oxidase-dependent two-wave cascade, *J. Neuroinflammation* 8 (2011) 129, <https://doi.org/10.1186/1742-2094-8-129>.
- [51] G. Gonzalez, J. Hodoň, A. Kazakova, C.W. D'Acunto, P. Kaňovský, M. Urban, M. Strnad, Novel pentacyclic triterpenes exhibiting strong neuroprotective activity in SH-SY5Y cells in salsolinol- and glutamate-induced neurodegeneration models, *Eur. J. Med. Chem.* 213 (2021) 113168, <https://doi.org/10.1016/j.ejmech.2021.113168>.
- [52] S. Kalimuthu, K. Se-Kwon, Cell survival and apoptosis signaling as therapeutic target for cancer: marine bioactive compounds, *Int. J. Mol. Sci.* 14 (2013) 2334–2354, <https://doi.org/10.3390/ijms14022334>.
- [53] M. Noguchi, N. Hirata, T. Tanaka, F. Suizu, H. Nakajima, J.A. Chiorini, Autophagy as a modulator of cell death machinery, *Cell Death Dis.* 11 (2020) 517, <https://doi.org/10.1038/s41419-020-2724-5>.
- [54] J. Zhu, A. Gusdon, H. Cimen, B. Houten, E. Koc, C. Chu, Impaired mitochondrial biogenesis contributes to depletion of functional mitochondria in chronic MPP+ toxicity: dual roles for ERK1/2, *Cell Death Dis.* 3 (2012) e312, <https://doi.org/10.1038/cddis.2012.46>.
- [55] J. Park, K.M. Jang, K.-K. Park, Effects of apamin on MPP+–Induced calcium overload and neurotoxicity by targeting CaMKII/ERK/p65/STAT3 signaling pathways in dopaminergic neuronal cells, *Int. J. Mol. Sci.* (2022), <https://doi.org/10.3390/ijms232315255>.
- [56] J. Park, K.M. Jang, Effects of Apamin on MPP(+)-Induced Calcium Overload and Neurotoxicity by Targeting CaMKII/ERK/p65/STAT3 Signaling Pathways in Dopaminergic Neuronal Cells, 23, 2022, <https://doi.org/10.3390/ijms232315255>.
- [57] S. Zhuang, G.R. Kinsey, Y. Yan, J. Han, R.G. Schnellmann, Extracellular signal-regulated kinase activation mediates mitochondrial dysfunction and necrosis induced by hydrogen peroxide in renal proximal tubular cells, *J. Pharmacol. Exp. Therapeut.* 325 (2008) 732–740, <https://doi.org/10.1124/jpet.108.136358>.
- [58] S.J. Fallon, O. Plant, Y.A. Tabi, S.G. Manohar, M. Husain, Effects of cholinesterase inhibition on attention and working memory in Lewy body dementias, *Brain Commun.* 5 (2023) fcad207, <https://doi.org/10.1093/braincomms/fcad207>.
- [59] E. d'Angremon, M.J.H. Begemann, T. van Laar, I.E.C. Sommer, Cholinesterase inhibitors for treatment of psychotic symptoms in alzheimer disease and Parkinson disease: a meta-analysis, *JAMA Neurol.* 80 (2023) 813–823, <https://doi.org/10.1001/jamaneurol.2023.1835>.
- [60] C. Truong, C. Recto, C. Lafont, F. Canoui-Poitrine, J.J. Belmin, C. Lafuente-Lafuente, Effect of cholinesterase inhibitors on mortality in patients with dementia, *Neurology* 99 (2022) e2313–e2325, <https://doi.org/10.1212/WNL.0000000000201161>.
- [61] Z. Luo, L. Liang, J. Sheng, Y. Pang, J. Li, L. Huang, X. Li, Synthesis and biological evaluation of a new series of ebselen derivatives as glutathione peroxidase (GPx) mimics and cholinesterase inhibitors against Alzheimer's disease, *Borg. Med. Chem.* 22 (2014) 1355–1361, <https://doi.org/10.1016/j.bmc.2013.12.066>.
- [62] A. Du, J. Xie, K. Guo, L. Yang, Y. Wan, Q. OuYang, X. Zhang, X. Niu, L. Lu, J. Wu, X. Zhang, A novel role for synaptic acetylcholinesterase as an apoptotic deoxyribonuclease, *Cell Discovery* 1 (2015) 15002, <https://doi.org/10.1038/celldisc.2015.2>.
- [63] L. Callén, E. Moreno, P. Barroso-Chinea, D. Moreno-Delgado, A. Cortés, J. Mallol, V. Casadó, J.L. Lanciego, R. Franco, C. Lluís, E.I. Canela, P.J. McCormick, Cannabinoid receptors CB1 and CB2 form functional heteromers in brain, *J. Biol. Chem.* 287 (2012) 20851–20865, <https://doi.org/10.1074/jbc.M111.335273>.
- [64] R. Ribeiro, J. Wen, S. Li, Y. Zhang, Involvement of ERK1/2, cPLA2 and NF- $\kappa$ B in microglia suppression by cannabinoid receptor agonists and antagonists, *Prostag. Other Lipid Mediat.* 100–101 (2013) 1–14, <https://doi.org/10.1016/j.prostaglandins.2012.11.003>.
- [65] F. Montecucco, V. Di Marzo, R.F. da Silva, N. Vuilleumier, L. Capetini, S. Lenglet, S. Pagano, F. Piscitelli, S. Quintao, M. Bertolotto, The activation of the cannabinoid receptor type 2 reduces neutrophilic protease-mediated vulnerability in atherosclerotic plaques, *Eur. Heart J.* 33 (2012) 846–856, <https://doi.org/10.1093/eurheartj/ehr449>.
- [66] D. Fernández-López, J. Martínez-Orgado, E. Nuñez, J. Romero, P. Lorenzo, M.Á. Moro, I. Lizaola, Characterization of the neuroprotective effect of the cannabinoid agonist WIN-55212 in an *in vitro* model of hypoxic-ischemic brain damage in newborn rats, *Pediatr. Res.* 60 (2006) 169–173, <https://doi.org/10.1203/01.pdr.0000228839.00122.6c>.

- [67] M. Aymerich, E. Rojo Bustamante, C. Molina, M. Celorrio, J.A. Sanchez Arias, R. Franco, Neuroprotective effect of JZL184 in MPP-treated SH-SY5Y cells through CB receptors, *Mol. Neurobiol.* 53 (2015), <https://doi.org/10.1007/s12035-015-9213-3>.
- [68] G. Fakhfour, A. Ahmadiani, R. Rahimian, A.A. Grolla, F. Moradi, A. Haeri, WIN55212-2 attenuates amyloid-beta-induced neuroinflammation in rats through activation of cannabinoid receptors and PPAR- $\gamma$  pathway, *Neuropharmacology* 63 (2012) 653–666, <https://doi.org/10.1016/j.neuropharm.2012.05.013>.
- [69] A. Quesada, B.Y. Lee, P.E. Micevych, PI3 kinase/Akt activation mediates estrogen and IGF-1 nigral DA neuronal neuroprotection against a unilateral rat model of Parkinson's disease, *Dev. Neurobiol.* 68 (2008) 632–644, <https://doi.org/10.1002/dneu.20609>.
- [70] V. Nogueira, Y. Park, C.C. Chen, P.Z. Xu, M.L. Chen, I. Tonic, T. Unterman, N. Hay, Akt determines replicative senescence and oxidative or oncogenic premature senescence and sensitizes cells to oxidative apoptosis, *Cancer Cell* 14 (2008) 458–470, <https://doi.org/10.1016/j.ccr.2008.11.003>.
- [71] J.S. Liou, C.-Y. Chen, J.S. Chen, D.V. Faller, Oncogenic ras mediates apoptosis in response to protein kinase C inhibition through the generation of reactive oxygen species, *J. Biol. Chem.* 275 (2000) 39001–39011, <https://doi.org/10.1074/jbc.M007154200>.
- [72] S. Maddika, S.R. Ande, E. Wiechec, L.L. Hansen, S. Wesselborg, M. Los, Akt-mediated phosphorylation of CDK2 regulates its dual role in cell cycle progression and apoptosis, *J. Cell Sci.* 121 (2008) 979–988, <https://doi.org/10.1242/jcs.009530>.
- [73] D. Trachootham, Y. Zhou, H. Zhang, Y. Demizu, Z. Chen, H. Pelicano, P.J. Chiao, G. Achanta, R.B. Arlinghaus, J. Liu, Selective killing of oncogenically transformed cells through a ROS-mediated mechanism by  $\beta$ -phenylethyl isothiocyanate, *Cancer Cell* 10 (2006) 241–252, <https://doi.org/10.1016/j.ccr.2006.08.009>.
- [74] G. Gonzalez, J. Grúz, C.W. D'Acunto, P. Kaňovský, M. Strnad, Cytokinin plant hormones have neuroprotective activity in in vitro models of Parkinson's disease, *Molecules* (2021), <https://doi.org/10.1016/j.ccr.2006.08.009>.
- [75] J. Cáceres-del-Carpio, M.T. Moustafa, J. Toledo-Corral, M.A. Hamid, S.R. Atilano, K. Schneider, P.S. Fukuhara, R.D. Costa, J.L. Norman, D. Malik, M. Chwa, D. S. Boyer, G.A. Limb, M.C. Kenney, B.D. Kuppermann, In vitro response and gene expression of human retinal Müller cells treated with different anti-VEGF drugs, *Exp. Eye Res.* 191 (2020) 107903, <https://doi.org/10.1016/j.exer.2019.107903>.
- [76] R.A. Carrasco, N.B. Stamm, B.K.R. Patel, One-step cellular Caspase-3/7 assay, *Biotechniques* 34 (2003) 1064–1067, <https://doi.org/10.2144/03345dd02>.
- [77] L. Rárová, J. Steigerová, M. Kvasnica, P. Bartůnek, K. Křížová, H. Chodounská, Z. Kolář, D. Sedlák, J. Oklestkova, M. Strnad, Structure activity relationship studies on cytotoxicity and the effects on steroid receptors of AB-functionalized cholestanes, *J. Steroid Biochem. Mol. Biol.* 159 (2016) 154–169, <https://doi.org/10.1016/j.jsbmb.2016.03.017>.
- [78] L. Rárová, Z. Pakulski, M. Strnad, M. Kvasnicová, T. Štenclová, P. Cmoch, Effect of modification of betulonic acid at the C3-carbon atom of homolupane triterpenoids on the antiproliferative activity in vitro, *J. Steroid Biochem. Mol. Biol.* 224 (2022) 106161, <https://doi.org/10.1016/j.jsbmb.2022.106161>.
- [79] G.M. Morris, R. Huey, W. Lindstrom, M.F. Sanner, R.K. Belew, D.S. Goodsell, A. J. Olson, AutoDock4 and AutoDockTools4: automated docking with selective receptor flexibility, *J. Comput. Chem.* 30 (2009) 2785–2791, <https://doi.org/10.1002/jcc.21256>.
- [80] O. Trott, A.J. Olson, AutoDock Vina: improving the speed and accuracy of docking with a new scoring function, efficient optimization, and multithreading, *J. Comput. Chem.* 31 (2010) 455–461, <https://doi.org/10.1002/jcc.21334>.
- [81] O. Hammer, D. Harper, P. Ryan, PAST: paleontological statistics software package for education and data analysis, *Palaeontol. Electron.* 4 (2001) 1–9, <https://doi.org/10.4236/cc.2021.91005>.